THE ASTROPHYSICAL JOURNAL, 225:357–379, 1978 October 15

COMPOSITIONS OF HALO CLUSTERS AND THE FORMATION OF THE GALACTIC HALO

LEONARD SEARLE AND ROBERT ZINN
Hale Observatories, Carnegie Institution of Washington, California Institute of Technology
Received 1978 March 2; accepted 1978 April 21

ABSTRACT

A new method of abundance determination, based upon reddening-independent characteristics of low-resolution spectral scans, has been applied to 177 red giants in 19 globular clusters. Most of these clusters have galactocentric distances exceeding 8 kpc. We find that there is no radial abundance gradient in the cluster system of the outer halo. The distribution over abundance for these outer clusters appears to be independent of galactocentric distance and is nearly identical to that for halo subdwarfs in the solar neighborhood. This distribution is such that the density declines exponentially with increasing metal abundance. The clusters of the outer halo show a broad spread in the color distribution on the horizontal branch, and this property is uncorrelated with metal abundance. In contrast, more tightly bound clusters, in the same range of abundance, show very little dispersion in this property. These facts are all consistent with the hypothesis that the loosely bound clusters of the outer halo have a broader range of age than the more tightly bound clusters and originated in transient protogalactic fragments that continued to fall into dynamical equilibrium with the Galaxy for some time after the collapse of its central regions had been completed.

Subject headings: clusters: globular — galaxies: Milky Way — galaxies: structure — stars: abundances — stars: late-type

I. INTRODUCTION

The structure of the globular-cluster system provides valuable clues to the dynamical and chemical history of the Galaxy, but, despite much work, even its qualitative features remain poorly known. For example, it does not appear to be known whether the range of abundances steadily diminishes with increasing galactocentric distance or whether there is some distance outside which the abundance gradient ceases. Although the latter situation might be anticipated if, as is widely believed, the metal-poor clusters formed from material that was freely falling during the galactic collapse, the effect does not seem to have been looked for, and, indeed, the available abundance determinations have been neither numerous enough nor sufficiently trustworthy to permit the discussion of such questions.

The lack of reliable abundance determinations also hampers progress in such problems as the interpretation of the "second parameter" that is needed to classify the color-magnitude diagrams of globular clusters. In particular, information on the galactic distribution of second-parameter effects has been lacking. Again, the distribution over abundance of the halo clusters is a clue to the chemical evolution of the protogalactic material and its determination, for a well-defined sample of clusters required more and better abundance estimates.

The work reported here was designed to make a substantial improvement in the quality and the quantity of abundance determinations, especially for the remote clusters of the outer halo. What is important for most of the questions that motivated this work is a reliable ranking of the clusters by abundance. The problem of providing a fundamental calibration of this abundance ranking is of secondary importance here.

Our work is based on observations of individual red giants, which, because of their intrinsic luminosities, can be observed in even the more distant clusters. We tackled the troublesome problem of interstellar reddening by devising a method of abundance ranking that makes use of reddening-independent characteristics of stellar spectra. We have developed a method that is sensitive to abundance even when the abundance is very low. In essence, what we measure is the line blocking in the blue region of the spectrum, obtained from low-resolution spectrum scans.

The ideas behind our method and the details of our observations and analysis are contained in §§ II–V. The abundance and reddening results are in §§ VI and VII, respectively. The general properties of the halo-cluster system inferred from these abundance results are discussed in § VIII. The purpose of our work was to throw some light on the formation of the Galaxy and its halo; these matters are discussed in § IX.

II. METHOD

Let S_i, $i = 1 \cdots n$, be a set of measurements of n intrinsic features of a red-giant spectrum. It is notationally convenient to regard these as the components

of a vector $\boldsymbol{S}$ which, we assume, will be determined by the star's effective temperature T, its surface gravity g, and its composition $\boldsymbol{X}$. The surface composition may, of course, require more than one parameter to specify it, and we intend by $\boldsymbol{X}$ to denote the vector of these parameters. We may express the dependence of $\boldsymbol{S}$ on its determining quantities by writing

$$(T, g, \boldsymbol{X}) : \boldsymbol{S}, \tag{1}$$

which is to be understood as indicating that the quantities in parentheses suffice in principle to determine the quantity $\boldsymbol{S}$. The relation (1) implicitly assumes that the atmospheric structure as well as the line and continuous absorption coefficients are determined by T, g, and $\boldsymbol{X}$. Specifically, we are assuming that effective gravity and microturbulent velocity are determined by these quantities.

If $\mathfrak{M}$ is the stellar mass and L its luminosity, then obviously

$$(\mathfrak{M}, L, T) : g, \tag{2}$$

and for red giants on the Hayashi line we have, in addition,

$$(L, \boldsymbol{X}) : T \tag{3}$$

and

$$(L, t, \boldsymbol{X}') : \mathfrak{M}, \tag{4}$$

where t is the age of the star and $\boldsymbol{X}'$ is the vector specifying the composition of the material from which the star formed. Implicit in relation (4) is the assumption that mass loss on the giant branch, if it occurs, is determined by the initial mass, t, and $\boldsymbol{X}'$. The assumptions made in these relations, if not certain, are not unreasonable. More problematic is our final assumption, namely, that $\boldsymbol{X} = \boldsymbol{X}'$. There is good evidence that red-giant stars in globular clusters sometimes have their atmospheres contaminated by the admixture of processed material from their interiors. We shall consider later the effects of mixing; for the moment we ignore it.

For unmixed stars, then, the relations (1) to (4) imply that

$$(L, \boldsymbol{X}, t) : \boldsymbol{S}. \tag{5}$$

A particular case of this relation is the assertion that L, $\boldsymbol{X}$, and t determine the star's bolometric correction, from which it follows that

$$(M_v, \boldsymbol{X}, t) : \boldsymbol{S}, \tag{6}$$

where M_v is the absolute visual magnitude of the star.

If then, for a particular observable S_i, we plot the representative point of a red giant in an (S_i, M_v)-diagram, the location of that point will be determined by the red giant's M_v, its age, and its composition. Observations of a homogeneous cluster of coeval stars will yield a sequence in the (S_i, M_v)-diagram. Two clusters of the same age but different compositions will give rise to different sequences if the observable S_i is suitably chosen. If we are dealing with globular clusters of nearly identical ages (as we shall assume), we may base abundance rankings on the relative location of these sequences in (S_i, M_v)-diagrams.

We turn now to the choice of a set of intrinsic, abundance-dependent parameters characterizing the spectral scans of red giants in globular clusters. In Figure 1 we have plotted twice a low-resolution spectral flux distribution of a typical globular-cluster red giant. In the upper panel the magnitude m is plotted against inverse wavelength. In the lower panel the same m is plotted instead against ψ where

$$\psi = 1.30\lambda^{-1} - 0.60, \quad \lambda^{-1} \leq 2.29,$$
$$\psi = 0.75\lambda^{-1} + 0.65, \quad \lambda^{-1} > 2.29. \tag{7}$$

This transformation, which is based upon the Whitford reddening law (Miller and Mathews 1972), has the advantage that areas defined by a flux distribution plotted in the (m, ψ)-plane are intrinsic (i.e., reddening-independent) parameters of the distribution. The observed flux distributions of red giants in the wavelength range $\lambda\lambda$5000–7500 are approximately linear in the (m, ψ)-plane, and a least-squares straight line through the observed points in this range is indicated in Figure 1. The magnitude deviations $Q(\lambda)$ of the observed points from this line are reddening-independent parameters of the stellar flux distribution, and a plot of Q against ψ is therefore a reddening-independent representation of this flux distribution and may be called the *intrinsic spectrum* of the star.

The intrinsic spectrum of a red giant in a globular cluster is determined, as we have shown, by the star's age, absolute visual magnitude, and composition. In Figure 2, observed flux distributions and the corresponding intrinsic spectra are illustrated for a typical red giant in each of four clusters. The clusters are arranged in order of increasing metal abundance from M92 to M71, and the stars chosen for this figure have closely similar absolute visual magnitudes (and, we assume, age), so that the differences among the intrinsic spectra illustrated in Figure 2 are due to the differences in the chemical composition of the clusters.

It is evident that the property that changes in the sequence of intrinsic spectra illustrated in Figure 2 is the integrated line absorption below λ5000. To the red of λ5000, either higher resolution or very high photometric precision would be needed to detect the very slight differences among these intrinsic spectra, whereas in the ultraviolet the differences are striking. The quantity $Q(3880)$, for example, changes by 1.5 mag for the abundance change between M92 and M71.

Our abundance rankings are therefore based upon the location of cluster sequences in the (S_i, M_v)-diagrams and the S_i are chosen to be some suitable functions of the $Q(\lambda)$ values for wavelengths less than λ5000. It is clear that the effects that we are measuring in these Q's are dominated by the line absorption of the common metals, although molecular band absorptions of CN and CH will also undoubtedly contribute. Fortunately, some of the Q's are expected to be more sensitive to molecular band absorption than

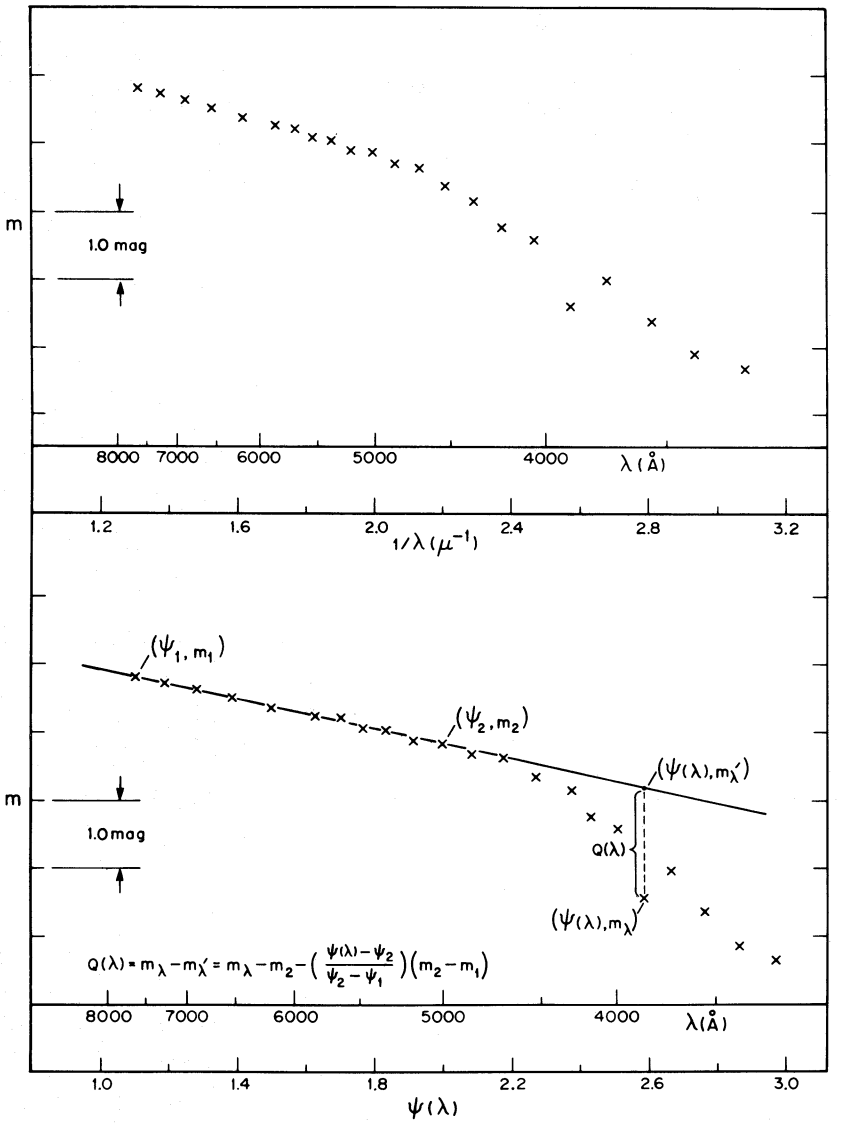

FIG. 1.—A low-resolution spectral flux distribution of a typical globular-cluster red giant. In the upper panel, flux per unit frequency interval, expressed as a magnitude, is plotted against frequency. In the lower panel, the same quantity is plotted against ψ, defined in the text. The figure defines and illustrates the geometrical significance of the reddening-free parameters $Q(\lambda)$.

others. In view of the possibility that the cluster abundances may require more than a single parameter to specify them, and of the fact that mixing effects are known to be important in some red-giant atmospheres, we shall need to investigate how well the rankings indicated by different S_i correlate. But first we shall describe the observational technique and the selection of the program clusters and stars.

III. TECHNIQUE AND PROGRAM

Individual red giants in the chosen clusters were observed with the multichannel spectrometer of the Hale 5 m reflector on Palomar Mountain. The instrument was used to measure the spectral flux density in 22 bands; of these, 16, with band centers located at λ3240 (160) λ5640, had a bandwidth of 160 Å, while the remaining six, centered at λ5820 (360) λ7620, had a 360 Å bandwidth. The bands were measured simultaneously and the time of integration was chosen so that the rms error due to photon statistics alone, in the λ3880 band, was always less than 0.05 mag and usually less than 0.03 mag. An individual observation consisted of at least two and usually four such integrations, and in most cases a particular star was observed on several nights.

The cluster fields are crowded. Observations were made through circular apertures of 5″, 7″, or 10″ diameter, whichever seemed appropriate under prevailing conditions. The spectrometer has two apertures, separated by 40″, for recording simultaneously

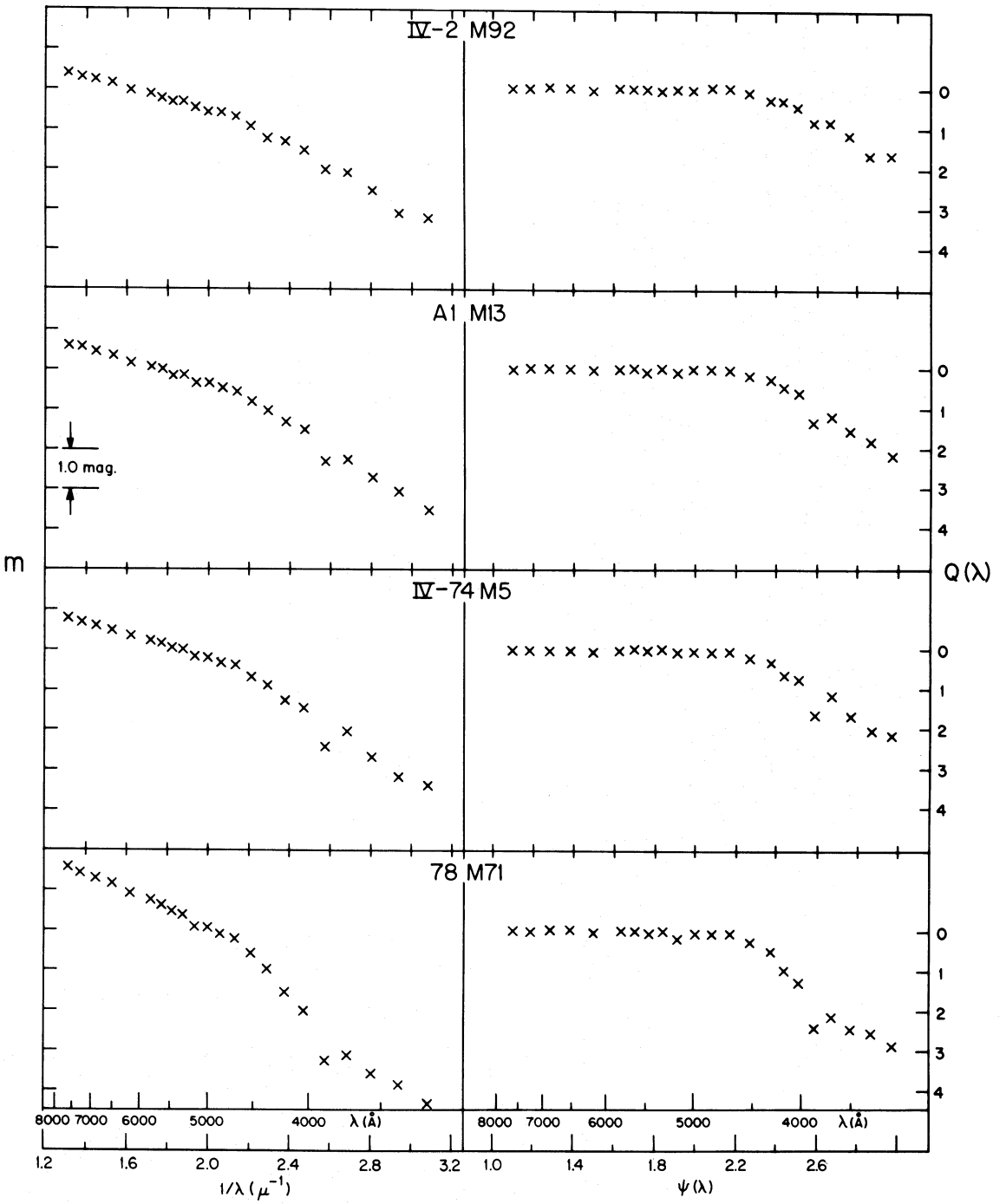

FIG. 2.—Spectral flux distributions and, in the right-hand panels, the corresponding intrinsic spectra are shown for a red giant in each of four different clusters. All these stars have $M_v \approx -1$, and the clusters are arranged, from top to bottom, in order of increasing metal abundance. The area between the observed distribution and the $Q = 0$ line increases with increasing metal abundance.

the spectrum of star-plus-sky and that of sky alone. One observation consisted of observing the star through each of these apertures; consequently, two sky positions, usually to the east and west of the star, were observed. The program stars were very carefully selected to ensure that good sky fields, free of bright stars, were available and that the star itself was uncontaminated. With the small apertures that we often wished to use, it became important to avoid errors resulting from differential refraction; observations were made at sufficiently small air masses that the seeing disk was comfortably enclosed in the aperture for all relevant wavelengths.

The flux densities were calibrated by means of observations of standard stars and reduced to absolute units (Oke and Schild 1970) by standard procedures. Intrinsic spectra were obtained in the manner earlier outlined. Specifically, we made a least-squares linear fit to the observations in the (m, ψ)-plane for the bands centered between λ5000 and λ7620 inclusive, but omitting the band centered at λ5160. (The λ5160 band is sensitive to the MgH and Mg I absorptions.) The deviations in magnitudes, $Q(\lambda)$, of the observed flux distribution from this fiducial continuum are the parameters of the intrinsic spectrum and are our basic observational data.

A program of 19 clusters was chosen, including all globular clusters north of 15° south declination that have galactocentric distances between 10 and 40 kpc and for which reliable color-magnitude diagrams are available. The choice of program stars was dictated by the need to avoid contamination in star and sky apertures and to obtain good absolute magnitude coverage for each cluster.

From their location in the color-magnitude array, the selected stars appeared to be cluster members on the giant branch, but a few, even so, turned out to be foreground stars, as we shall discuss in § IV. A few asymptotic giant-branch stars were added to the program, and, for clusters where detailed spectroscopy has been carried out, we were careful to include giants that exhibit the full range of CH and CN band strength that is found within a cluster.

The 177 stars for which successful observations were made are listed in Table 1. The stars are arranged by cluster in order of increasing R.A. The star designation, V, and $B - V$ come from the reference cited. The value of M_v results from the cluster distance modulus, which is here obtained from the assumption that the horizontal branch in the vicinity of the RR Lyrae gap is at $M_v = +0.6$. Column (8) indicates the number of nights on which each star was observed. The quantity Ψ is the observed color gradient or red slope of the energy distribution expressed as the magnitude difference of the fiducial continuum between λ5000 and λ8000. The values of $Q(\lambda)$ are the reddening-independent parameters of the energy distribution. To keep Table 1 from being too bulky, the values of Q are tabulated for seven wavelengths only. We omitted the ultraviolet bands between λ3240 and λ3720, which had somewhat larger errors than the rest and which did not add any information not already contained in the retained Q's. We also omitted bands which, for all stars, yielded very small values of Q, values not significantly different from zero. It may be useful to remark that, from the values of Ψ and $Q(\lambda)$ that are given in Table 1, the raw observed stellar flux distribution can be recovered. The average errors in Ψ and in the $Q(\lambda)$ values were estimated from the numerous multiple observations. The error estimates that are appropriate to an individual observation are given in the last row of Table 1.

IV. ELIMINATION OF FIELD STARS

To make sure that our sample of cluster giants is as free as possible from contamination by field stars, we eliminated from it all stars that failed to meet three distinct criteria. In the first place, for acceptance, a star must lie on the giant branch in the cluster's color-magnitude array. A few stars that fail to meet this criterion were intentionally included on our observing program; these are asymptotic giant-branch stars and are denoted by AGB in Table 1. Since color-magnitude arrays are of varying qualities and some clusters are located in star-rich fields, this

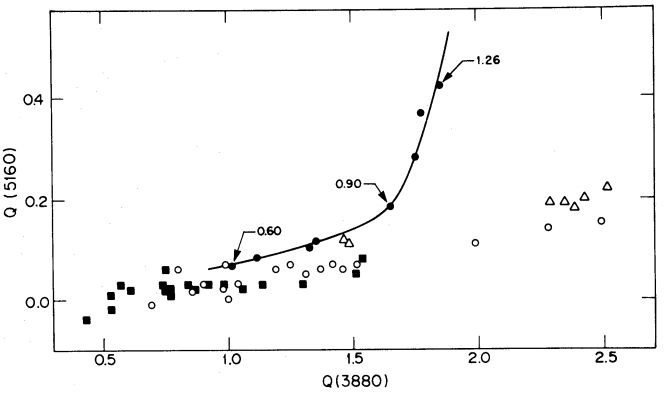

FIG. 3.—Foreground dwarf stars, masquerading as cluster red giants, can be distinguished from cluster members in this diagram. Squares, open circles, and triangles are individual red giants in the clusters M92, M13, and M71, respectively. Closed circles are Pleiades dwarfs, and $B - V$ values are indicated for three of these. Foreground dwarfs are expected to lie near the dwarf sequence and, for $B - V \geq 0.9$, will be well separated from the globular-cluster red giants of all abundances.

1978ApJ...225..357S

TABLE 1

OBSERVATIONAL DATA

(1) NGC	(2) M	(3) Star	(4) V	(5) B-V	(6) ref	(7) M_V	(8) n	(9) Ψ	(10) Q(5160)	(11) Q(4840)	(12) Q(4680)	(13) Q(4520)	(14) Q(4360)	(15) Q(4200)	(16) Q(4040)	(17) Q(3880)	(18) S	(19) Remarks
4147		I-10	16.98	0.79	1	0.73	1	0.82	0.07	0.01	-0.02	0.13	0.17	0.34	0.35	0.89	0.25	
		I-19	16.43	0.84	1	0.18	1	0.79	0.01	0.01	-0.02	0.08	0.16	0.31	0.35	0.88	0.23	
		II-7	16.72	0.81	1	0.47	1	0.86	0.02	-0.06	-0.02	0.09	0.15	0.32	0.35	0.88	0.23	
		II-8	16.83	0.82	1	0.58	1	0.73	0.03	0.02	0.06	0.12	0.28	0.36	0.47	0.96	0.30	
		II-10	15.73	1.03	1	-0.52	2	0.92	0.04	0.05	0.06	0.20	0.41	0.62	0.64	1.46	0.46	field ?
		II-14	15.26	1.01	1	-0.99	1	0.99	0.05	0.08	0.10	0.20	0.36	0.52	0.77	1.37	0.46	
		IV-6	16.78	0.87	1	0.53	2	0.83	0.02	0.00	0.03	0.12	0.19	0.32	0.44	0.89	0.27	
		IV-13	15.02	1.08	1	-1.23	2	1.11	0.05	0.04	0.05	0.19	0.25	0.49	0.63	1.32	0.40	
5024	53	P	14.81	1.09	2	-1.56	2	1.06	0.06	0.04	0.07	0.19	0.24	0.46	0.58	1.12	0.36	
		M	14.57	1.15	2	-1.80	2	1.14	0.07	0.05	0.06	0.22	0.28	0.52	0.64	1.27	0.41	
		G	14.10	1.42	2	-2.27	2	1.34	0.10	0.08	0.11	0.28	0.40	0.69	0.87	1.63	0.55	
		X	15.61	0.95	2	-0.76	2	0.92	0.05	0.02	0.03	0.14	0.18	0.37	0.45	0.91	0.28	
		K	13.77	1.58	2	-2.60	1	1.50	0.12	0.11	0.17	0.38	0.53	0.87	1.09	1.91	0.68	
5053		42	15.23	0.89	3	-0.80	1	0.97	0.03	-0.01	-0.02	0.17	0.14	0.31	0.33	0.79	0.23	
		O	15.57	0.97	3	-0.46	2	0.93	0.05	0.04	0.00	0.14	0.22	0.39	0.50	0.98	0.30	field ?
		C	13.98	1.11	3	-2.05	2	1.20	0.07	0.06	0.08	0.23	0.26	0.47	0.66	1.13	0.39	
		24	15.65	0.74	3	-0.38	2	0.78	0.04	0.01	-0.01	0.09	0.06	0.26	0.29	0.62	0.17	
		D	14.48	1.01	3	-1.55	1	1.08	0.06	0.05	0.08	0.19	0.24	0.40	0.71	1.01	0.36	
5272	3	1397	12.65	1.56	4	-2.38	2	1.57	0.18	0.13	0.12	0.37	0.53	0.92	1.33	2.18	0.75	
		297	12.89	1.42	4	-2.14	2	1.44	0.13	0.09	0.10	0.30	0.43	0.83	1.15	2.11	0.67	
		BF	13.62	1.16	5	-1.41	2	1.12	0.08	0.03	0.02	0.19	0.29	0.54	0.78	1.43	0.44	
		AE	13.85	0.98	5	-1.18	2	1.09	0.08	-0.01	-0.03	0.15	0.18	0.37	0.54	1.17	0.32	AGB
		L	15.15	0.83	5	0.12	2	0.83	0.06	-0.02	-0.02	0.11	0.17	0.33	0.43	0.98	0.26	
		T	14.62	0.77	5	-0.41	2	0.82	0.05	0.02	-0.03	0.09	0.08	0.25	0.38	0.90	0.22	AGB
		AV	14.01	1.04	5	-1.02	1	1.02	0.03	0.03	0.03	0.14	0.25	0.46	0.60	1.39	0.39	
		I-III-28	12.81	1.37	4	-2.22	2	1.42	0.12	0.06	0.07	0.27	0.38	0.69	0.99	1.77	0.57	
		I-IV-25	13.60	1.13	5	-1.43	2	1.14	0.08	0.01	0.03	0.18	0.27	0.50	0.73	1.51	0.43	
		I-IV-27	13.99	1.00	5	-1.04	2	1.05	0.07	0.02	0.01	0.17	0.22	0.48	0.64	1.42	0.39	
5466		Y	14.10	1.11	6	-1.88	2	1.14	0.06	0.07	0.06	0.20	0.23	0.47	0.63	1.21	0.39	
		G	13.63	1.37	6	-2.35	2	1.34	0.09	0.10	0.12	0.31	0.43	0.71	0.94	1.64	0.57	
		S	14.78	0.93	6	-1.20	1	0.90	0.14	0.00	-0.06	0.07	0.24	0.47	0.53	1.37	0.34	field
		S4R3-18	14.93	0.94	6	-1.05	2	0.96	0.07	0.01	0.03	0.17	0.21	0.36	0.60	0.97	0.31	
		S4R3-25	14.58	0.95	6	-1.40	2	1.00	0.06	0.01	0.01	0.16	0.17	0.34	0.51	0.94	0.29	
		S4R4-1	16.17	0.79	6	0.19	1	0.77	0.04	0.00	0.02	0.13	0.21	0.29	0.38	0.79	0.24	
PAL 5		F	15.96	1.07	7	-0.81	1	1.13	0.06	0.06	0.04	0.18	0.30	0.56	0.69	1.58	0.46	
		G	15.95	1.02	7	-0.82	2	1.07	0.07	0.08	0.05	0.23	0.33	0.62	0.71	1.66	0.49	
		K	16.51	0.96	7	-0.26	1	1.04	0.06	0.05	0.04	0.17	0.29	0.53	0.65	1.44	0.42	
		N	16.78	0.96	7	0.01	1	0.98	0.06	0.04	0.05	0.20	0.32	0.56	0.68	1.47	0.44	
		M	16.73	0.79	7	-0.04	1	0.84	0.06	0.00	0.00	0.14	0.17	0.29	0.34	0.73	0.22	AGB ?
		O	16.78	0.82	7	0.01	1	0.72	0.13	0.01	-0.01	0.12	0.25	0.43	0.49	1.27	0.34	field ?
		E	15.73	1.03	7	-1.04	2	1.15	0.08	0.10	0.07	0.29	0.40	0.66	0.78	1.62	0.53	

TABLE 1—*Continued*

(1) NGC	(2) M	(3) Star	(4) V	(5) B-V	(6) ref	(7) M_V	(8) n	(9) Ψ	(10) Q(5160)	(11) Q(4840)	(12) Q(4680)	(13) Q(4520)	(14) Q(4360)	(15) Q(4200)	(16) Q(4040)	(17) Q(3880)	(18) S	(19) Remarks
5904	5	I-4	13.27	1.18	8	-1.24	1	1.12	0.09	0.06	0.05	0.27	0.37	0.64	0.80	1.63	0.51	
		I-71	13.05	1.21	8	-1.46	1	1.17	0.13	0.10	0.10	0.31	0.40	0.77	0.92	1.94	0.61	
		I-74	14.02	0.96	8	-0.49	1	0.99	0.08	0.07	0.07	0.21	0.31	0.53	0.94	1.38	0.47	
		II-93	14.31	0.93	8	-0.20	1	0.93	0.06	0.09	0.06	0.23	0.29	0.56	0.89	1.46	0.48	
		III-50	12.88	1.24	8	-1.63	1	1.13	0.07	0.09	0.07	0.27	0.33	0.65	0.79	1.72	0.53	AGB
		III-78	12.60	1.45	8	-1.91	2	1.40	0.14	0.12	0.13	0.32	0.49	0.88	1.23	2.10	0.71	
		IV-26	13.60	0.93	8	-0.91	2	0.92	0.06	0.08	0.06	0.19	0.26	0.46	0.71	1.24	0.40	AGB
		IV-59	12.68	1.30	8	-1.83	1	1.25	0.11	0.12	0.14	0.33	0.47	0.88	1.18	2.14	0.71	
		IV-74	13.50	1.10	8	-1.01	1	1.05	0.06	0.06	0.05	0.27	0.37	0.64	0.80	1.63	0.51	
		429	14.91	0.67	8	0.40	1	0.57	0.03	0.06	0.01	0.14	0.09	0.24	0.53	0.67	0.23	HB
		469	14.60	0.92	8	0.09	1	0.89	0.07	0.07	0.07	0.17	0.21	0.45	0.77	1.29	0.41	
		IV-19	12.57	1.43	8	-1.94	2	1.38	0.15	0.14	0.13	0.33	0.50	0.89	1.21	2.15	0.72	
6171	107	17	15.13	1.33	9	0.10	1	1.42	0.15	0.15	0.10	0.25	0.45	0.72	0.84	1.85	0.59	
		117	15.63	1.29	9	0.60	1	1.52	0.07	0.09	0.04	0.21	0.31	0.58	0.63	1.53	0.45	
		205	14.58	1.46	9	-0.45	1	1.66	0.16	0.14	0.07	0.31	0.39	0.80	0.89	1.97	0.61	
		J	13.97	1.55	9	-1.06	1	1.80	0.13	0.14	0.10	0.32	0.47	0.84	1.02	2.08	0.67	
6205	13	A10	14.33	0.88	4	-0.02	2	0.89	0.03	-0.01	-0.03	0.10	0.24	0.34	0.49	1.04	0.29	
		A1	13.39	1.05	4	-0.96	2	1.07	0.05	0.01	0.01	0.16	0.37	0.46	0.61	1.31	0.39	
		J37	14.52	0.84	10	0.17	2	0.85	0.00	-0.02	-0.02	0.10	0.21	0.29	0.50	1.00	0.27	
		K422	14.02	0.97	11	-0.33	2	0.89	0.06	0.03	0.04	0.17	0.27	0.45	0.61	1.19	0.37	
		A95	14.12	0.73	12	-0.23	2	0.80	0.01	-0.02	-0.04	0.08	0.22	0.24	0.36	0.77	0.21	AGB
		A371	12.95	1.09	12	-1.40	2	1.14	0.07	0.04	0.03	0.20	0.39	0.56	0.71	1.52	0.46	
		X24	13.75	0.95	4	-0.60	1	0.93	0.07	0.04	0.02	0.16	0.22	0.42	0.53	1.25	0.35	
		13	13.49	0.84	13	-0.86	2	0.88	0.03	-0.01	-0.02	0.10	0.20	0.29	0.37	0.91	0.24	AGB
		J50	14..60	0.88	10	0.25	1	0.80	0.07	0.04	0.01	0.14	0.22	0.35	0.42	0.99	0.29	
		J3	13.31	1.06	10	-1.04	1	1.04	0.07	0.03	0.03	0.19	0.25	0.48	0.62	1.42	0.40	
		B651	13.17	1.07	12	-1.18	3	1.08	0.06	0.03	0.02	0.19	0.31	0.52	0.63	1.46	0.42	
		A171	12.84	1.03	12	-1.51	2	1.12	0.06	0.04	0.03	0.19	0.31	0.50	0.65	1.37	0.41	AGB
		J45	14.98	0.76	10	0.63	2	0.77	0.02	0.01	0.01	0.12	0.17	0.32	0.44	0.98	0.27	
		A462	15.69	0.69	14	1.34	1	0.73	0.02	-0.03	0.00	0.05	0.06	0.23	0.56	0.87	0.23	
		A455	15.98	0.57	14	1.63	2	0.60	0.06	0.02	0.04	0.14	0.15	0.29	0.49	0.80	0.26	
		B818	14.06	0.68	12	-0.29	1	0.82	-0.01	-0.06	-0.06	0.04	0.29	0.17	0.30	0.69	0.18	AGB
		3	12.04	1.61	13	-2.31	1	1.54	0.14	0.17	0.21	0.44	0.64	1.10	1.32	2.28	0.83	
		III-63	12.20	1.39	15	-2.15	1	1.36	0.11	0.13	0.15	0.35	0.50	0.88	1.09	1.99	0.68	
		IV-25	12.09	1.54	15	-2.26	1	1.57	0.15	0.19	0.23	0.46	0.66	1.16	1.48	2.49	0.90	
6229		I-9	15.84	1.27	16	-1.66	2	1.19	0.09	0.08	0.09	0.29	0.43	0.77	0.93	1.84	0.59	
		I-11	16.62	0.99	16	-0.88	2	0.93	0.04	0.04	0.03	0.16	0.21	0.43	0.54	1.28	0.36	
		I-18	15.96	1.22	16	-1.54	2	1.22	0.08	0.08	0.04	0.22	0.38	0.68	0.87	1.81	0.54	
		II-13	17.16	1.00	16	-0.34	2	0.95	0.05	-0.02	0.00	0.16	0.27	0.44	0.57	1.41	0.38	
		II-19	16.45	0.87	16	-1.05	1	0.70	0.16	0.02	0.03	0.14	0.39	0.66	0.68	1.78	0.49	field
		III-19	16.31	1.08	16	-1.19	2	1.04	0.07	0.03	0.01	0.23	0.31	0.54	0.67	1.54	0.45	
		III-21	15.93	1.21	16	-1.57	1	1.14	0.41	0.07	-0.04	0.16	0.42	0.86	0.94	2.11	0.60	field
		IV-12	15.15	1.33	16	-2.35	2	1.36	0.13	0.11	0.12	0.37	0.50	0.91	1.11	2.20	0.71	

1978ApJ...225..357S

TABLE 1—*Continued*

(1) NGC	(2) M	(3) Star	(4) V	(5) B-V	(6) ref	(7) M_V	(8) n	(9) Ψ	(10) Q(5160)	(11) Q(4840)	(12) Q(4680)	(13) Q(4520)	(14) Q(4360)	(15) Q(4200)	(16) Q(4040)	(17) Q(3880)	(18) S	(19) Remarks
6254	10	F	11.93	1.75	17	-2.12	3	1.97	0.17	0.20	0.20	0.44	0.58	0.96	1.17	2.07	0.76	
		K	12.40	1.48	17	-1.57	2	1.66	0.11	0.14	0.11	0.27	0.44	0.82	0.89	1.90	0.61	
		I-63	13.18	1.15	17	-0.87	3	1.26	0.06	0.09	0.05	0.21	0.29	0.46	0.51	1.14	0.37	AGB
		I-68	14.39	1.00	17	0.34	1	1.09	0.06	0.11	0.08	0.22	0.25	0.44	0.56	1.10	0.37	
		I-113	13.36	1.29	17	-0.69	1	1.37	0.09	0.11	0.07	0.20	0.29	0.50	0.60	1.46	0.44	
		I-166	13.77	1.17	17	-0.28	1	1.38	0.05	0.05	0.02	0.12	0.22	0.42	0.48	1.21	0.34	
		I-170	13.32	1.27	17	-0.73	1	1.33	0.07	0.11	0.10	0.23	0.36	0.58	0.64	1.35	0.45	
		I-173	12.84	1.27	17	-1.21	1	1.48	0.06	0.11	0.02	0.22	0.31	0.52	0.53	1.29	0.40	AGB
		I-222	12.80	1.36	17	-1.25	2	1.54	0.08	0.13	0.13	0.28	0.43	0.67	0.82	1.54	0.54	
		II-44	11.87	1.60	17	-2.18	2	1.73	0.18	0.20	0.19	0.42	0.59	0.97	1.19	2.16	0.77	
6341	92	I-22	15.31	0.70	18	0.82	1	0.73	-0.02	-0.01	-0.01	0.09	0.10	0.21	0.12	0.53	0.14	
		II-6	15.07	0.73	18	0.58	2	0.79	0.02	-0.05	-0.04	0.07	0.13	0.20	0.28	0.61	0.16	
		II-24	14.54	0.74	18	0.05	1	0.79	0.06	0.00	-0.01	0.13	0.16	0.31	0.29	0.75	0.22	
		II-70	13.03	0.98	18	-1.46	2	1.07	0.03	0.03	0.01	0.16	0.18	0.39	0.49	0.98	0.30	
		III-4	14.12	0.71	18	-0.37	3	0.78	0.03	-0.03	-0.03	0.07	0.14	0.20	0.25	0.57	0.15	AGB
		III-13	12.05	1.46	18	-2.44	4	1.45	0.08	0.07	0.10	0.28	0.36	0.65	0.83	1.54	0.51	
		III-65	12.36	1.18	18	-2.13	2	1.27	0.03	0.04	0.04	0.20	0.25	0.51	0.65	1.30	0.40	
		III-81	14.38	0.59	18	-0.11	1	0.74	0.01	-0.06	-0.06	0.05	0.15	0.15	0.35	0.53	0.14	AGB
		IV-2	13.49	0.92	18	-1.00	5	0.99	0.02	0.00	-0.01	0.11	0.19	0.32	0.42	0.88	0.25	
		IV-10	13.43	0.94	18	-1.06	3	1.02	0.03	0.01	0.00	0.14	0.23	0.34	0.46	0.92	0.28	
		IV-114	13.84	0.83	18	-0.65	3	0.91	0.03	0.01	0.01	0.13	0.21	0.31	0.46	0.84	0.26	
		V-45	12.81	1.03	18	-1.68	2	1.13	0.02	0.03	0.02	0.19	0.21	0.43	0.53	1.06	0.33	
		VI-7	13.59	0.66	18	-0.90	1	0.72	0.03	-0.03	-0.05	0.07	0.30	0.23	0.30	0.80	0.22	field ?
		VI-18	13.79	0.79	18	-0.73	3	0.89	0.03	0.00	-0.02	0.12	0.17	0.27	0.39	0.74	0.22	AGB
		VII-10	13.71	0.81	18	-0.78	2	0.86	0.02	0.01	-0.01	0.12	0.12	0.30	0.39	0.77	0.23	AGB
		VII-18	12.14	1.33	18	-2.35	3	1.36	0.05	0.07	0.09	0.26	0.36	0.63	0.80	1.51	0.50	
		IX-6	14.62	0.76	18	0.13	2	0.79	0.01	0.02	-0.01	0.15	0.14	0.29	0.41	0.77	0.24	
		IX-10	14.64	0.74	18	0.15	2	0.78	0.02	0.02	0.00	0.14	0.13	0.29	0.44	0.76	0.24	
		IX-12	14.51	0.58	18	0.02	1	0.66	-0.04	-0.03	-0.08	0.00	0.31	0.09	0.28	0.43	0.13	AGB
		XII-8	12.74	1.03	18	-1.75	2	1.14	0.03	0.02	0.04	0.17	0.20	0.38	0.48	0.99	0.31	AGB
6779	56	E-22	13.78	1.32	19	-1.92	3	1.53	0.07	0.09	0.07	0.26	0.32	0.60	0.83	1.51	0.49	
		E-27	14.23	1.18	19	-1.47	1	1.20	0.17	0.10	0.08	0.25	0.42	0.79	0.90	1.90	0.59	field
		E-32	14.75	1.03	19	-0.95	1	1.17	0.18	0.10	0.10	0.25	0.47	0.81	0.89	2.02	0.62	field
		E-35	14.43	0.99	19	-1.27	3	1.33	0.06	0.07	0.05	0.20	0.26	0.48	0.64	1.25	0.40	
		E-40	15.07	0.88	19	-0.63	2	1.21	0.03	0.03	0.01	0.13	0.12	0.31	0.38	0.84	0.24	
		E-61	13.48	1.31	19	-2.22	1	1.22	0.13	0.09	0.09	0.25	0.43	0.82	1.08	2.11	0.65	field ?
6838	71	23	15.06	1.17	20	1.16	2	1.14	0.12	0.11	0.05	0.22	0.35	0.52	0.70	1.47	0.46	
		46	12.34	1.82	20	-1.56	2	2.08	0.20	0.05	-0.01	0.21	0.52	0.98	1.33	2.43	0.73	
		77	12.71	1.83	20	-1.19	2	2.00	0.22	0.07	0.05	0.25	0.63	1.01	1.44	2.52	0.79	
		78	12.87	1.59	20	-1.03	2	1.57	0.18	0.07	0.08	0.27	0.60	0.98	1.31	2.39	0.76	
		79	14.08	1.46	20	0.18	3	1.38	0.25	0.11	0.19	0.34	0.59	1.12	1.35	2.50	0.83	field ?
		C	14.49	1.17	20	0.59	4	1.16	0.11	0.07	0.05	0.19	0.35	0.54	0.74	1.49	0.46	HB
		S	13.10	1.52	20	-0.80	4	1.64	0.19	0.09	0.10	0.32	0.53	0.97	1.16	2.35	0.74	
		Y	13.93	1.28	20	0.03	2	1.19	0.23	0.09	0.10	0.27	0.45	0.82	1.06	2.15	0.66	field ?
		A9	13.10	1.57	20	-0.80	2	1.79	0.19	0.06	0.08	0.28	0.59	0.92	1.24	2.29	0.73	

TABLE 1—*Continued*

(1) NGC	(2) M	(3) Star	(4) V	(5) B-V	(6) ref	(7) M_V	(8) n	(9) Ψ	(10) Q(5160)	(11) Q(4840)	(12) Q(4680)	(13) Q(4520)	(14) Q(4360)	(15) Q(4200)	(16) Q(4040)	(17) Q(3880)	(18) S	(19) Remarks
6934		I-4	14.88	1.12	21	-1.34	2	1.30	0.07	0.06	0.06	0.25	0.33	0.66	0.81	1.78	0.53	
		I-84	16.15	1.06	21	-0.07	2	1.00	0.05	0.02	0.15	0.17	0.25	0.44	0.51	1.15	0.36	
		I-90	15.16	1.15	21	-1.06	2	1.25	0.06	0.06	0.05	0.21	0.32	0.55	0.69	1.45	0.45	
		I-109	14.05	1.56	21	-2.17	2	1.78	0.18	0.16	0.17	0.41	0.61	1.11	1.41	2.53	0.86	
		II-32	14.55	1.27	21	-1.67	2	1.41	0.09	0.07	0.07	0.26	0.38	0.75	0.95	1.92	0.59	
		II-36	15.52	1.03	21	-0.70	2	1.05	0.04	0.04	0.03	0.17	0.21	0.41	0.53	1.17	0.34	AGB
		II-47	14.69	1.20	21	-1.53	2	1.32	0.08	0.08	0.06	0.25	0.37	0.70	0.88	1.82	0.56	
6981	72	16	14.66	1.25	22	-1.63	2	1.26	0.08	0.07	0.07	0.26	0.37	0.72	0.88	1.91	0.57	
		17	14.95	1.14	22	-1.34	2	1.10	0.10	0.11	0.09	0.25	0.37	0.65	0.79	1.56	0.51	
		18	14.86	1.21	22	-1.43	2	1.20	0.10	0.11	0.11	0.32	0.43	0.78	0.91	1.95	0.62	
		19	16.11	0.82	22	-0.18	4	0.79	0.07	0.08	0.02	0.16	0.17	0.36	0.41	0.95	0.29	
		29	15.93	0.86	23	-0.36	2	0.82	0.06	0.07	0.02	0.12	0.17	0.35	0.41	1.00	0.29	
		47	15.29	1.06	23	-1.00	2	1.07	0.07	0.06	0.03	0.21	0.27	0.57	0.69	1.59	0.46	
		64	14.46	1.32	23	-1.83	2	1.33	0.12	0.12	0.11	0.33	0.47	0.87	1.03	2.10	0.68	
		88	16.28	0.90	23	-0.01	1	0.81	0.07	0.06	0.08	0.21	0.27	0.47	0.56	1.24	0.39	
		110	15.81	0.95	23	-0.48	1	0.98	0.03	0.02	-0.01	0.16	0.23	0.49	0.55	1.38	0.38	
		12	14.58	1.26	23	-1.71	1	1.31	0.08	0.07	0.06	0.27	0.42	0.77	0.97	1.98	0.61	
7006		II-28	16.77	1.24	24	-1.43	2	1.28	0.06	0.07	0.07	0.26	0.34	0.62	0.77	1.71	0.52	
		II-46	16.38	1.38	24	-1.82	2	1.32	0.09	0.11	0.08	0.29	0.42	0.77	0.92	1.94	0.61	
		II-69	17.59	0.98	24	-0.61	1	1.04	0.10	0.09	0.04	0.22	0.33	0.51	0.58	1.38	0.42	
		II-103	16.23	1.41	24	-1.97	2	1.47	0.12	0.11	0.15	0.40	0.54	0.97	1.19	2.31	0.76	
		III-1	16.44	1.37	24	-1.76	1	1.39	0.38	0.08	0.06	0.14	0.36	0.86	1.01	2.38	0.65	field
		III-5	16.73	1.01	24	-1.47	1	0.90	0.22	-0.01	-0.01	0.18	0.33	0.55	0.65	1.68	0.45	field
		III-7	17.97	0.90	24	-0.23	2	1.00	0.05	-0.07	0.05	0.22	0.22	0.47	0.47	1.21	0.35	
		III-33	16.77	1.10	24	-1.43	3	1.13	0.07	0.09	0.07	0.24	0.32	0.59	0.71	1.42	0.46	
		III-46	16.78	1.24	24	-1.42	3	1.22	0.06	0.07	0.09	0.24	0.37	0.64	0.80	1.60	0.51	
		III-55	17.95	0.93	24	-0.25	1	0.79	0.23	0.11	0.07	0.19	0.40	0.64	0.73	1.81	0.53	field
7078	15	II-75	13.01	1.26	4	-2.25	4	1.41	0.05	0.07	0.08	0.26	0.38	0.60	0.86	1.42	0.49	
		S37	15.27	0.83	4	+0.01	4	0.89	0.03	0.02	0.02	0.11	0.14	0.29	0.46	0.74	0.24	
		S6	13.35	1.21	4	-1.91	5	1.30	0.05	0.06	0.06	0.23	0.32	0.54	0.81	1.31	0.45	
		P6	14.95	0.90	4	-0.31	5	0.98	0.02	0.02	-0.01	0.12	0.12	0.30	0.44	0.79	0.24	
		P7	15.59	0.79	4	+0.33	2	0.87	-0.01	0.02	-0.03	0.10	0.07	0.25	0.36	0.71	0.20	
		P13	14.32	0.98	4	-0.94	5	1.09	0.03	0.00	0.00	0.13	0.19	0.33	0.54	0.86	0.27	
		X6	14.11	1.01	4	-1.15	3	1.09	0.02	0.00	0.00	0.13	0.25	0.33	0.54	0.92	0.29	
		X2	14.62	0.97	4	-0.64	1	1.09	0.03	-0.02	0.01	0.11	—	0.32	0.52	0.82	—	
		S23	14.01	1.04	4	-1.25	1	1.01	0.09	-0.06	-0.03	0.12	0.46	0.50	0.79	1.53	0.44	field

TABLE 1—*Continued*

(1) NGC	(2) M	(3) Star	(4) V	(5) B−V	(6) ref	(7) M_V	(8) n	(9) Ψ	(10) Q(5160)	(11) Q(4840)	(12) Q(4680)	(13) Q(4520)	(14) Q(4360)	(15) Q(4200)	(16) Q(4040)	(17) Q(3880)	(18) S	(19) Remarks
7089	2	I-511	14.90	0.91	25	−0.55	2	1.01	0.03	0.01	0.00	0.17	0.23	0.47	0.55	1.34	0.37	
		I-576	13.54	1.33	25	−1.91	5	1.35	0.12	0.12	0.11	0.33	0.46	0.83	1.04	1.99	0.66	
		I-574	15.64	0.85	25	+0.19	2	0.91	0.00	0.00	−0.03	0.15	0.16	0.35	0.36	1.07	0.28	
		A	13.15	1.55	25	−2.30	2	1.47	0.11	0.09	0.10	0.33	0.45	0.86	1.15	2.06	0.67	
		I-20	15.20	0.93	25	−0.25	3	0.91	0.02	0.01	−0.02	0.15	0.16	0.37	0.45	1.16	0.30	
		I-2	14.12	1.15	25	−1.33	3	1.13	0.09	0.08	0.08	0.28	0.39	0.67	0.86	1.65	0.54	
		I-190	13.71	1.21	25	−1.74	3	1.19	0.10	0.11	0.12	0.32	0.41	0.70	1.02	1.74	0.59	
		I-240	14.25	1.22	25	−1.20	2	1.04	0.12	0.15	0.13	0.36	0.60	1.05	1.00	2.19	0.74	field ?
		I-298	14.03	1.18	25	−1.42	3	1.20	0.06	0.04	0.04	0.22	0.31	0.59	0.78	1.63	0.48	
		S	13.79	1.20	25	−1.66	2	1.21	0.10	0.11	0.08	0.29	0.42	0.69	0.98	1.65	0.57	
		I-395	14.46	1.03	25	−0.99	3	1.08	0.06	0.06	0.03	0.22	0.30	0.56	0.74	1.53	0.46	
		I-254	14.04	1.13	25	−1.41	1	1.12	0.07	0.06	0.06	0.24	0.34	0.63	0.95	1.69	0.53	
		—	—	—	—	—	—	0.03	0.02	0.05	0.05	0.05	0.05	0.04	0.09	0.06	0.02	
		σ																

primary criterion is, by itself, inadequate; we have supplemented it by two spectroscopic ones.

We noticed that in some stars the λ5211 band of MgH, as measured by $Q(5160)$, was stronger than in otherwise similar stars of the same cluster. For stars redder than $(B-V)_0 \sim 0.9$, the strength of this band depends on surface gravity being stronger in dwarfs than in giants. Figure 3 shows a plot of $Q(5160)$ against $Q(3880)$ for stars that we believe to be members of M13, M71, and M92 and also for a selection of Pleiades dwarfs. We rejected from our sample stars that deviated from their cluster sequence in this diagram. The rejected stars are indicated in Table 1 with the notation "field." Since, as can be seen from Figure 3, this criterion fails to discriminate among the bluer stars of our program, we imposed the third selection criterion.

Since $Q(3880)$ and Ψ are both functions of the composition, age, and absolute visual magnitude of a star (see relation [6] of § II), a plot of these two quantities against one another should produce a tight sequence. Field stars that do not share the same composition, age, and absolute visual magnitude are expected to deviate from this cluster sequence. Figure 4 illustrates the usefulness of such a plot for detecting field stars that meet the MgH criterion for membership. Since Ψ is not a reddening-independent quantity, we run the risk of eliminating genuine cluster members that happen to be anomalously reddened, but this is not of concern for our purposes. More seriously, we may eliminate genuine cluster members that have anomalous surface compositions. We cannot rule out this possibility, but too few stars are involved to affect the general conclusions of this paper. Stars that met the MgH criterion but failed to meet the $Q(3880)$, Ψ test are regarded as probable field stars and are denoted by "field?" in Table 1.

References for Table 1

1. Sandage and Walker 1955.
2. Cuffey 1965.
3. Sandage, Katem, and Johnson 1977.
4. Sandage 1970.
5. Johnson and Sandage 1956.
6. Cuffey 1961.
7. Sandage and Hartwick 1977.
8. Arp 1962.
9. Dickens and Rolland 1972.
10. Arp and Johnson 1955.
11. Kadla 1966.
12. Osborn 1971*b*.
13. Baum 1954.
14. Savedoff 1956.
15. Cathey 1974.
16. Zinn, unpublished.
17. Harris, Racine, and de Roux 1976.
18. Sandage and Walker 1966.
19. Barbon 1965.
20. Arp and Hartwick 1971.
21. Harris and Racine 1973.
22. Dickens 1972, Table 1.
23. Dickens 1972, Table 2.
24. Sandage and Wildey 1967.
25. Harris 1975.

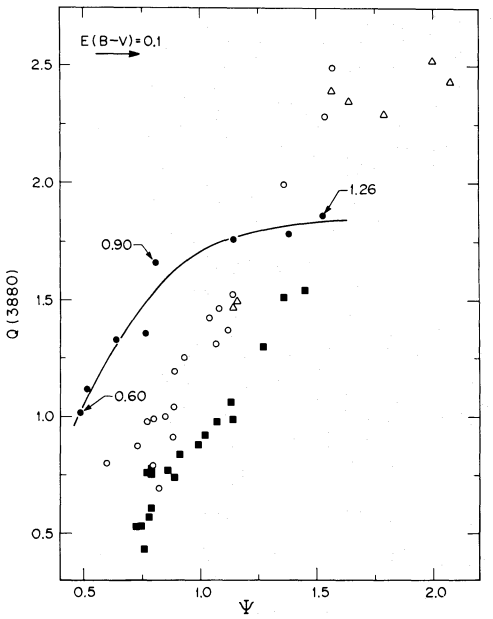

FIG. 4.—Foreground dwarfs with $B - V \leq 0.9$ can be distinguished from red-giant cluster members in this diagram. Symbols have the same significance as in Fig. 3 and Ψ is the slope of the red continuum, defined in the text. Taken together, Figs. 3 and 4 provide a means of eliminating foreground dwarfs from our sample.

We have no reason to doubt that the remaining stars are genuine cluster members, and it is upon their spectra that our abundance ranking will be based.

V. WHAT ABUNDANCES ARE WE MEASURING?

Our basic data are the values of $Q(\lambda)$ given in Table 1. They are reddening-free measures of the line blocking in a number of 160 Å bands. The line blocking clearly depends on the relative abundances of numerous elements, but the main factor common to all bands is undoubtedly the ratio of the abundance of the iron peak elements to that of hydrogen. The question is whether this ratio is the only thing that matters. Since strong spectral features due to calcium and to the CH and CN molecules fall within some of the bands, the observations may also give information on the Ca/Fe, C/Fe, and N/Fe ratios; other effects are probably insignificant at this resolution. We cannot avoid considering the sensitivity of our observations to such secondary abundance effects.

a) CN *and* CH *Variations within Clusters*

A number of studies (see McClure and Norris 1977; Zinn 1977, and references therein) have shown that the G band (i.e., the λ4310 CH band) and the CN bands show variations from star to star in some globular clusters. These variations are widely thought to result from convective mixing of material from the stellar interiors.

The G band lies within our λ4360 band. Since Norris and Zinn (1977) found that G-band variations in M13 and in M92 produced a change of only 0.1 mag in the flux through a 22 Å filter centered on the band, it is not to be expected that the effects on our broader bands will be very noticeable. We have plotted $Q(4360)$ against Ψ for the stars in M13, M15, M92, and M5; some of these have been identified in the papers cited above as weak G-band stars. This exercise confirmed that G-band variations of the magnitude observed in clusters cannot be detected at our resolution. As Figure 2 shows, the $Q(4360)$ band is sensitive to the general metal abundance, however.

The CN bands at λ4216 and λ3883 contribute to the values of $Q(4200)$ and $Q(3880)$, respectively. A CH star, or an extreme CN star, like those found in ω Centauri (see, e.g., Dickens and Bell 1976; Bessell and Norris 1976) would certainly have substantially larger values of $Q(4200)$ and $Q(3880)$ than a normal giant. Only one of our 177 stars seems likely to be a star of this type. This is I-240 in M2, which we have designated as a possible field star but which could well be a strong CN cluster member. The more typical CN variations, such as those that Osborn (1971*a*) and Zinn (1977) discovered among the giants in M5, have only small effects on our measurements. This is shown in Figure 5; $Q(4200)$ and $Q(3880)$ are affected by CN absorption while $Q(4520)$ is not, but the known CN stars do not deviate from the general trend in any of these diagrams. Clearly, the blocking measured by $Q(4200)$ and by $Q(3880)$ is dominated by the common metals even in stars where CN is known to be exceptionally strong.

b) *Secondary Abundances and the Second Parameter*

There may be systematic differences among the clusters in the abundances of C, N, and O (see, e.g., Cohen, Frogel, and Persson 1978). Such differences may be responsible for the differences among clusters in some characteristics of their color-magnitude arrays. Sandage and Wildey (1967) found that the cluster NGC 7006 has a paucity of blue horizontal-branch stars, unlike other clusters of similar metal abundance, and Hartwick and McClure (1972) reported that four of its red giants had spectra with exceptionally strong CN bands. They suggested that N/Fe is unusually large in this cluster and that this abundance peculiarity might be responsible for the anomalous color distribution on the horizontal branch. In view of the evidence that has since accumulated for CN variations within clusters, this case looks rather less convincing now than it did at the time that it was made. More work needs to be done on the problem to investigate whether the four stars studied by Hartwick and McClure are truly representative. For our purposes, it suffices to show that the effect is not apparent in our data.

As will be shown later, NGC 7006 and M2 have the same metal abundance, within the accuracy of our measurements. Unlike NGC 7006, however, M2 possesses a blue horizontal branch (Arp 1955). If this second-parameter effect is related to N/Fe differences, as Hartwick and McClure suggest, a comparison of these two clusters might show the effects of differing

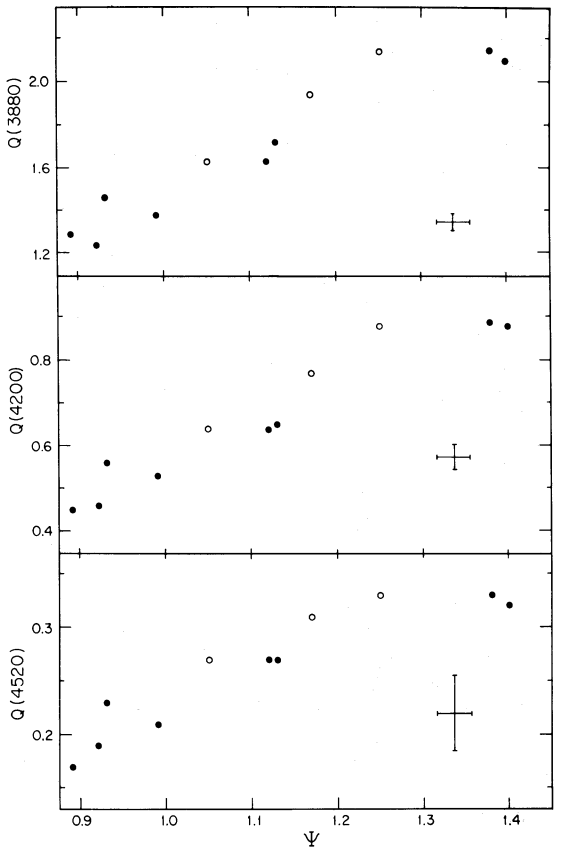

FIG. 5.—Observations of red giants in M5 illustrate the insensitivity of our measurements to the differences known to exist in the strength of the CN bands among the stars of this cluster. Closed circles are normal red giants; open circles are stars whose spectra are known to have anomalously strong CN bands. $Q(3880)$ and $Q(4200)$ monitor bands that contain important CN band heads; $Q(4520)$ monitors a band free from CN absorption. The line blocking in all bands increases as the stellar continuum becomes redder, but the behavior of the strong CN stars is not different from that of the normal giants.

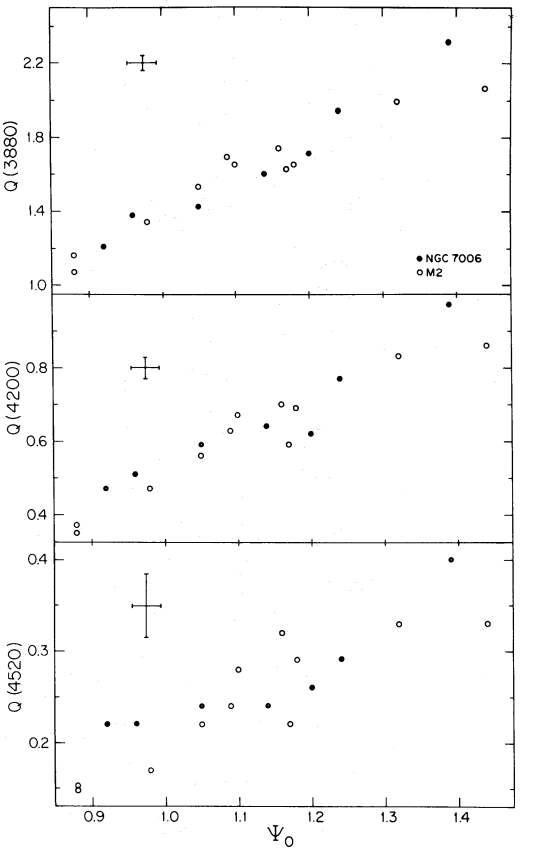

FIG. 6.—The same Q's as in Fig. 5 plotted against the de-reddened continuum slope for the stars in two clusters. It has been suggested that the N/Fe ratio is larger in NGC 7006 than it is in normal clusters of the same metal abundance such as M2. The two clusters cannot be distinguished from one another in any of these three diagrams. If the N/Fe ratio really is different in the two clusters, then our observations are insensitive to such differences.

N/Fe ratios on our measurements. In Figure 6 we plot, as before, $Q(4520)$, $Q(4200)$, and $Q(3880)$ against the unreddened color Ψ_0 for the stars that we have observed in these two clusters. Whether we consider the band at $\lambda(4520)$, which is free from CN contamination, or the two bands at $\lambda 3880$ and $\lambda 4200$, which are strongly contaminated by CN absorption, we find the same result; namely, that NGC 7006 and M2 have the same abundances. Either N/Fe is the same in both clusters or our system is insensitive to such N/Fe differences as exist.

c) *The Choice of a Spectral Characteristic*

The fact is that all the $Q(\lambda)$ values, for λ between $\lambda 3880$ and $\lambda 4840$, are extremely highly correlated. We have been unable to devise anything more complex than a one-parameter abundance classification for these clusters. Cohen (1978) has recently shown, from a high-dispersion study of red giants in M13 and M3, that the relative abundance of some elements actually does vary from cluster to cluster. It is clear, however, that the measurements reported here are dominated by one abundance parameter and that this is the ratio of the common metals to hydrogen. That this is so is supported by the agreement of our results (see § VI) with Cohen's value of [Fe/H] for M3 and M13 and with Butler's (1975) results obtained from measurements of the Ca K line in the spectra of cluster variables.

Since our observations determine only one parameter, we should like to reduce our Q values to one summarizing value. Examining the intrinsic spectra of Figure 2, it seemed natural to adopt a measure that was related to the area below the $Q = 0$ line in these diagrams. To use a measure that could conveniently be expressed in magnitudes, it seemed natural to use

a weighted mean of the individual Q values. These considerations led us to adopt

$$S = \sum_i w_i Q(\lambda_i) \Big/ \sum_i w_i , \qquad (8)$$

where the sums are taken over the bands from λ3880 to λ4840, inclusive, and w_i is the bandwidth of each of the 160 Å bands expressed in units of ψ. For each star a value of S is given in column (18) of Table 1. Our abundance ranking is based on the sequences that are defined by a cluster's red giants in the (S, M_v)-plane.

VI. THE ABUNDANCE RANKING

In Figure 7 the intrinsic spectral parameter S is plotted against M_v for red giants in four well-studied clusters. Each cluster defines a tight sequence, and the sequences are well displaced from one another, with the more metal-abundant clusters having larger S values at a given absolute visual magnitude. A family of smooth free-hand curves have been drawn through the data points. Similar curves were constructed for each cluster and, from them, the value of S was read off at $M_v = -1$. This value we shall call $\langle S \rangle$. It is specific to an individual cluster and is determined essentially by observation of red giants

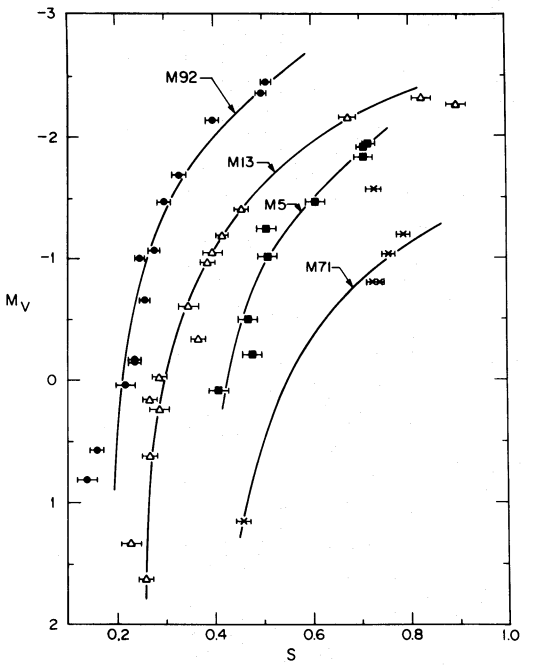

FIG. 7.—The reddening-independent spectral parameter S plotted against absolute magnitude for the red giants in four clusters. The lines drawn are simply eye fits to the observations. The stars in each cluster define a tight sequence and the sequences are well separated. Line blocking is more severe in the more metal-rich clusters. Our abundance ranking is based on the location of cluster sequences in this diagram.

with absolute visual magnitudes in the range $-2 \leq M_v \leq 0$. It is well determined for all the clusters included in this paper. Values of $\langle S \rangle$ for each cluster, together with its estimated error, are given in Table 2; these values summarize our observations.

The estimated error in $\langle S \rangle$ given in column (10) of Table 2 is that resulting from photometric errors and from any abundance dispersion within a cluster. Another possible source of error arises from the values of M_v that were adopted. These values are given in Table 1 and are based on the assumption that $\langle M_v \rangle = +0.6$ for the horizontal branch in the vicinity of the RR Lyrae gap in each cluster (Sandage 1970). This choice has the advantage that the values of M_v assigned to the giants do not depend on knowledge of the interstellar reddening. Our procedure in this way maintains its reddening-independent character. The possibility remains, however, that the value of $\langle M_v \rangle$ for the horizontal branch actually differs from cluster to cluster. If this value is strictly correlated with the metal abundance in the cluster, then clearly such differences will leave our abundance rankings unaffected and they can be ignored. In the worst case, where differences in horizontal-branch absolute magnitudes exist but are uncorrelated with abundance, the estimates of $\langle S \rangle$ will be subject to an extra source of "random" error. As an upper limit to the possible intrinsic spread of $\langle M_v \rangle$ for the horizontal branch, we have adopted ± 0.2 mag from a consideration of Graham's (1975, 1977) photometry of the RR Lyrae variables in the Magellanic Clouds. This translates into a possible additional random error of ± 0.02 in $\langle S \rangle$ if our worst-case assumptions actually apply. We conclude that the error in the determination of $\langle S \rangle$ is dominated by observational scatter and that uncertainties in the absolute magnitudes of the horizontal branch can, for our purposes, safely be ignored.

The location of a cluster sequence in the (S, M_v)-plane is dependent both on abundance and cluster age; it is necessary to consider the errors that might arise in an abundance ranking based on the parameter $\langle S \rangle$ that ignores a possible age spread among clusters. A large part of the change in $\langle S \rangle$ with abundance results from the shift in the effective temperature of the red-giant sequence. At $M_v = -1$, a change in effective temperature amounting to $\Delta T_e \sim 300$ K results from a change in abundance by a factor of 10. The changes in effective temperature resulting from age differences at constant abundances are, in comparison, very small. From the work of Ciardullo and Demarque (1977), we find $\Delta T_e \sim 25$ K for the age difference between 9 and 16 billion years. We conclude that ignoring the age differences that may exist among the globular clusters may produce errors in our abundance estimates but that these are unlikely to exceed ± 0.05 in [Fe/H].

In Figure 8, $\langle S \rangle$ is plotted against Butler's (1975) determinations of [Fe/H] for the clusters common to the two investigations. Butler's [Fe/H] values are based upon the strength of the K line in the spectra of cluster RR Lyrae stars. Figure 8 shows that apart

1978ApJ...225..357S

TABLE 2

THE COMPOSITION OF THE CLUSTERS

(1) NGC	(2) $(m-M)_V$	(3) E(B-V)	(4) D⊙	(5) X	(6) Y	(7) Z	(8) r	(9) ⟨ S ⟩	(10) σ	(11) [Fe/H]	(12) σ
4147	16.25	0.02[b]	17.3	-1.3	-3.7	16.8	19.8	0.38	±0.03	-1.64	±0.11
5024	16.37	0.00[b]	18.8	2.9	-1.5	18.5	19.4	0.30	0.02	-1.93	0.07
5053	16.03	0.01[b]	15.8	2.7	-1.3	15.5	16.6	0.27	0.02	-2.05	0.07
5272	15.03	0.01[b]	10.0	1.5	1.4	9.8	12.1	0.37	0.02	-1.67	0.07
5466	15.98	0.00[b]	15.7	3.4	3.1	15.0	16.1	0.30	0.02	-1.93	0.07
PAL 5	16.75	0.03[b]	21.4	15.1	0.3	15.1	16.5	0.52	0.02	-1.11	0.07
5904	14.51	0.01[a]	7.9	5.4	0.4	5.8	6.6	0.51	0.02	-1.15	0.07
6171	15.03	0.31[c]	6.3	5.8	0.3	2.5	3.7	0.67	0.05	-0.55	0.19
6205	14.35	0.02[b]	7.2	2.8	4.7	4.7	8.8	0.39	0.02	-1.60	0.07
6229	17.50	0.00[a]	31.6	7.1	23.2	20.3	30.8	0.43	0.02	-1.45	0.07
6254	14.05	0.25[b]	4.4	3.8	1.0	1.9	5.2	0.48	0.02	-1.26	0.07
6341	14.49	0.02[b]	7.7	2.4	5.8	4.4	9.6	0.28	0.02	-2.01	0.07
6779	15.70	0.20[a]	10.2	4.7	8.9	1.6	9.8	0.33	0.04	-1.82	0.15
6838	13.90	0.27[c]	4.0	2.2	3.3	-0.4	7.1	0.76	0.02	-0.22	0.07
6934	16.22	0.11[a]	14.8	8.6	11.1	-4.8	12.1	0.45	0.02	-1.37	0.07
6981	16.29	0.00[a]	18.1	12.4	8.7	-9.9	13.7	0.44	0.03	-1.41	0.11
7006	18.20	0.05[a]	40.5	16.8	34.4	-13.2	37.7	0.43	0.03	-1.45	0.11
7078	15.26	0.08[a]	10.0	3.8	8.1	-4.5	10.4	0.30	0.02	-1.93	0.07
7089	15.45	0.02[b]	11.9	5.7	7.8	-7.0	10.9	0.43	0.02	-1.45	0.07

[a] The reddening determined by the technique discussed in the text.

[b] The reddening given by either Table 1 of Burstein and McDonald (1975) or the reference listed in Table 1 of this paper. Our technique confirms these values.

[c] The reddening given by Table 1 of Burstein and McDonald (1975). It was not possible to check these values by our technique.

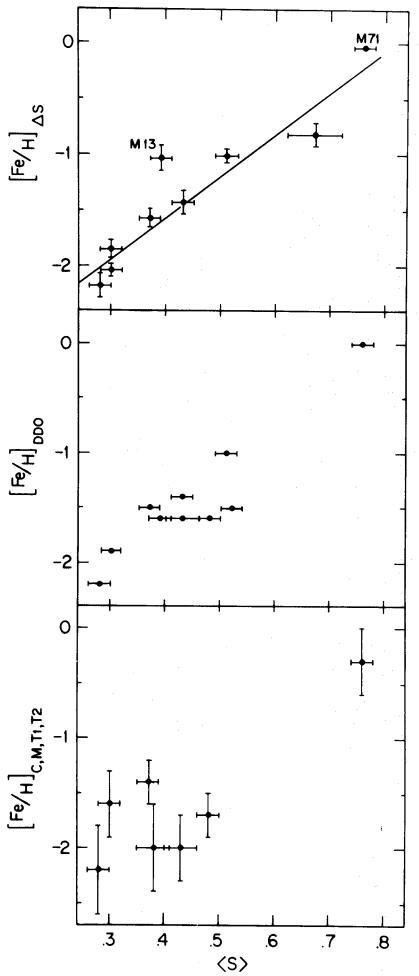

FIG. 8.—The ranking parameter $\langle S \rangle$ plotted against estimates of [Fe/H] obtained in other investigations. From top to bottom, the plots concern the work of Butler (1975), Hesser, Hartwick, and McClure (1977), and Canterna (1975). The line drawn in the upper panel is the relation that we have provisionally adopted to give a rough scale to our rankings. The intrinsic relation between [Fe/H] and $\langle S \rangle$ is, of course, unlikely to be linear.

from M13 the two rankings are in excellent agreement. The value Butler determined for M71 is more uncertain than others, since it is based on observations of one star of dubious membership. Ignoring the points for M13 and M71, the points in Figure 8 are well fitted by the relation

$$[\mathrm{Fe/H}] = 3.73\langle S \rangle - 3.05 . \qquad (9)$$

This line is shown in Figure 8.

An entirely independent check on our abundance ranking is given by comparison with DDO photometry. The [Fe/H] estimates of Hesser, Hartwick, and McClure (1977) depend on the adoption of values of [Fe/H] for M92, M3, and for the pair of clusters M71 and NGC 6352; the values adopted are −2.2, −1.5, and 0.0, respectively. In the second panel of Figure 8 we have plotted the values of [Fe/H] obtained by Hesser *et al.* against $\langle S \rangle$. There is good general agreement, and it is particularly interesting that there is no discrepancy between our data and the indications of DDO photometry for the cluster M13. There are, however, numerous disagreements in the detailed rankings.

Finally, in the bottom panel of Figure 8, our values of $\langle S \rangle$ are plotted against the values of [Fe/H] derived from the C, M, T_1, T_2 system by Canterna (1975). This system is calibrated via analyzed field stars and theoretical colors. Like DDO photometry, it has the weakness that it requires the interstellar reddening to be known. The scatter in this diagram shows the insensitivity and lack of precision of the C, M, T_1, T_2 system, whose abundance estimates are based on broad-band filter photometry to the red of λ4500. The reason for this lack of sensitivity, particularly at low abundance levels, is clear from a consideration of the intrinsic spectra of globular-cluster red giants illustrated in Figure 2.

A fundamental calibration of the ranking parameter, $\langle S \rangle$, in terms of [Fe/H] will only become available as a result of high-dispersion, curve-of-growth studies of individual red giants in globular clusters. In the meantime, to give a rough scale to our rankings we adopt the relation of equation (9). The values of [Fe/H] derived from $\langle S \rangle$ and this relation are given in Table 2, together with an estimate of the associated random errors. From Cohen's work fundamental [Fe/H] values are now known for two clusters; for M3 and M13 she finds values of −1.8 and −1.6, respectively. Our values for these two clusters are −1.7 and −1.6.

Turning now to the question of the chemical homogeneity of globular clusters, we emphasize once again that, in our observational program, we have included stars known to have anomalously weak G bands and others known to have anomalously strong CN bands as compared with other stars at the same M_v in the same clusters. We have shown that our measurements are insensitive to these effects. The question here is: How homogeneous are these clusters in the abundance level of the common metals?

We find that the scatter of the observed points in the (S, M_v)-diagrams, such as those in Figure 7, can in all cases be entirely attributed to the estimated observational errors of an S measurement. If we attribute *all* the scatter, nevertheless, to a dispersion in the abundance of the common metals, we shall clearly derive a cautious upper limit.[1] We find that, in all cases

$$\sigma([\mathrm{Fe/H}]) < 0.13 , \qquad (10)$$

and we emphasize that there is no evidence whatever from our data favoring inhomogeneity of metal abundance within any cluster.

[1] It should be remembered, however, that this result concerns stars on the outer fringes of the clusters, which are the only ones that we observed.

VII. THE REDDENING OF THE CLUSTERS

Since the color, Ψ, of the red continuum is a spectral characteristic, the considerations of § II lead one to expect that the (M_v, Ψ)- and the (S, Ψ)-diagrams would contain abundance information. The difficulty is, of course, that the measured values of Ψ are not intrinsic parameters, being subject to the effects of interstellar reddening. If one attempts to perform an abundance ranking from the location of the cluster sequences in these two diagrams, it becomes clear that the effects of reddening are important and produce ranking errors of opposite sense in the two diagrams. This can clearly be turned to advantage.

We found from the literature those clusters having well-determined values of $E(B - V) \leq 0.05$; we shall refer to these as the fiducial clusters. We made the small corrections to Ψ that were appropriate to obtain the unreddened value Ψ_0 and found that the fiducial clusters gave consistent abundance rankings in the (M_v, S)-, in the (M_v, Ψ_0)-, and in the (S, Ψ_0)-diagrams. For the remaining clusters we adjusted $E(B - V)$ by trial and error, until the rankings in the (M_v, Ψ_0)- and (S, Ψ_0)-diagrams came into agreement with that previously obtained from the reddening-independent (M_v, S)-diagram. The values of $E(B - V)$ that resulted from this procedure are listed in Table 2. Two clusters, NGC 6171 and NGC 6838, are more metal-rich than any of the fiducial clusters and the method just described could not be applied to them.

Apart from the distance modulus and the reddening and abundance information, Table 2 also contains data concerning the location of the clusters; all distances are in kiloparsecs. Columns (4) and (8) contain the heliocentric and galactocentric distances which assume a distance of 8.5 kpc for the Sun's distance from the galactic center, while columns (5), (6), and (7) contain heliocentric rectangular coordinates, with Z perpendicular to the galactic plane and X the direction toward the galactic center.

VIII. CHARACTERISTICS OF THE CLUSTER SYSTEM

The main properties of the Galaxy's system of globular clusters have been reviewed by Woltjer (1975) and Harris (1976). The clusters are distributed with approximate spherical symmetry about the galactic center. There is no evidence for any disk component to the system. The most metal-rich clusters are apparently *not* concentrated to the galactic plane. Globular clusters with metal abundances that are greater than 1/10 of the solar abundance are confined to a region within 8 kpc of the galactic center. We shall refer to this region as the inner halo.

The aim of this investigation is to clarify the properties of the cluster system of the outer halo (i.e., $r > 8$ kpc), and to discuss these properties in the light of conflicting ideas concerning the formation of the Galaxy. We have determined abundances and have either determined or checked the reddening estimates, and hence distances, for 15 clusters of the outer halo. This brings to 16 the number of such clusters with well-determined properties. Rough but quantitative abundance estimates are available for a number of other clusters in the outer halo from the work of Kukarkin (1974). There are 13 of these, not yet studied in detail, that have galactic latitudes exceeding 15°, so that their estimated distances are not seriously in doubt as a result of extinction uncertainties. In all, then, we have distance and abundance measurements for a sample of 16 and reasonable estimates for a further 13 clusters with $r > 8$ kpc. It is from these data that we shall try to infer the main characteristics of the cluster system of the outer halo.

a) Is There an Abundance Gradient in the Outer Halo?

There is no doubt that the mean metal abundance of the globular clusters of the inner halo is greater than that of the clusters of the outer halo; the work of Mayall (1946), Morgan (1956), and Kinman (1959) established the point. What is not so clear, however, is that the mean metal abundance decreases monotonically with increasing galactocentric distance, at all distances. Do we find only extremely metal-poor clusters at large distances?

The evidence relating to this question is shown in Figure 9. Here we have plotted abundance against galactocentric distance for the 19 clusters of our survey and for 25 other clusters that have galactic latitude exceeding 15° and for which distances are available from Harris (1976). Only four of these have first-class abundance determinations; for the remainder we have used the estimates of Kukarkin (1974). Judging by the intercomparison of our own abundance determinations and Kukarkin's estimates, the latter are not in error by much more than ± 0.2 in [Fe/H] despite their derivation from heterogeneous data.

Figure 9 shows that there is a great range of abundance at all galactocentric distances in the halo and no evidence at all that the mean abundance decreases with increasing galactocentric distance outside 8 kpc. The usual nonparametric statistical tests show that the distribution over abundance for clusters in the range $8 \leq r \leq 15$ and in the range $r > 15$ are compatible with the hypothesis that these distributions result from random sampling of a single parent distribution. In any case, it is certainly *not* true that one finds only extremely metal-poor clusters at large galactocentric distances.

This result was surprising to us, since Sandage (1969) had given evidence for a correlation between kinematics and abundance for very metal-poor subdwarfs. To investigate this question, Sandage had divided his sample into two ultraviolet-excess groups. It seemed possible that this binning might have included some subdwarfs of the inner halo in the more metal-rich group. We wondered whether the result might be modified if we rebinned so as to eliminate a few of the more metal-rich stars. To do this, we divided Sandage's sample into two excess groups with $0.18 \leq \delta(U - B) < 0.25$ and $\delta(U - B) \geq 0.25$. This corresponds, according to the calibration of Wallerstein (1962), to abundance ranges $-1.0 \geq$ [Fe/H] > -1.8 and [Fe/H] ≤ -1.8, and yields two

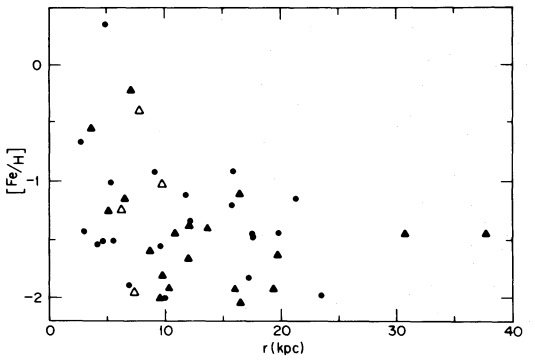

FIG. 9.—Abundances plotted against galactocentric distance for all clusters with tolerable estimates of both quantities. The solid triangles are the clusters studied in this paper. Open triangles are other clusters with first-rate abundance determinations. The circles represent clusters for which the abundance estimates were taken from Kukarkin (1974). Outside $r = 8$ kpc, the distribution over abundance does not change significantly with galactocentric distance.

groups with 29 and 20 stars, respectively. Applying a Kolmogorov-Smirnov test at the 10% significance level, we find no reason to reject the hypothesis that the distributions over U, V, or W velocities for these two samples are simply the result of random sampling from the same parent distributions. The same can be said of the distribution over apogalactic distance inferred from the Bottlinger diagram. We conclude that there is no statistically significant evidence that the kinematics of subdwarfs more metal-poor than 1/10 of the solar metal abundance are correlated with their abundances.

The indications of Figure 9 are supplemented by qualitative evidence regarding the metal abundance in very remote globular clusters obtained by Cowley, Hartwick, and Sargent (1978). Their spectral classifications of individual red giants, belonging to 12 clusters and dwarf spheroidal systems, in the range of galactocentric distances between 30 and 100 kpc, indicate that there is a range of abundances at all distances—a range that is similar to that observed for clusters with distances between 10 and 20 kpc.

In the absence of any compelling theoretical reason for supposing a gradient to exist, we draw the tentative conclusion that for $r > 8$ kpc the distribution over abundance of halo globular clusters is independent of galactocentric distance.

b) The Second Parameter and Galactic Structure

It is well known that the distribution over color of the stars on the horizontal branches of the color-magnitude arrays of globular clusters is only loosely correlated with the clusters' metal abundances. Much previous work (van den Bergh 1967; Sandage and Wildey 1967) has shown that a second parameter besides metal abundance is involved in determining the morphology of the color-magnitude arrays. Whatever the nature of this second parameter, it is of interest to see in what way it is related to the location of the clusters in the globular-cluster system.

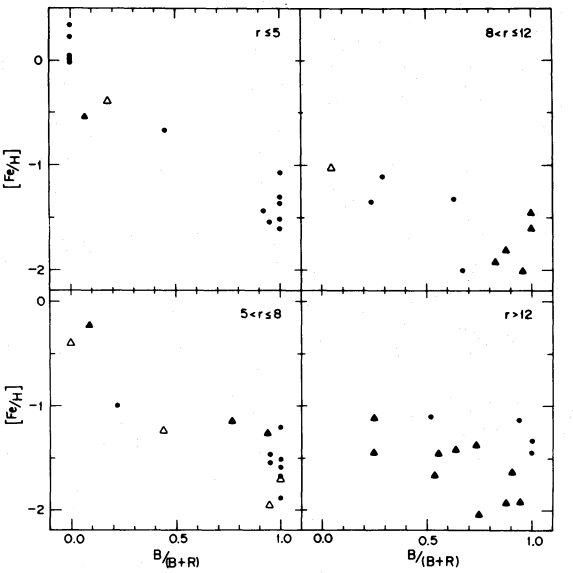

FIG. 10.—For all clusters with $r < 40$ kpc and for which color-magnitude diagrams exist, abundance is plotted against a parameter measuring the color distribution of the horizontal-branch stars. The four panels refer to clusters located in different intervals of galactocentric distance. The symbols are as in Fig. 9. The figure shows that, for clusters of the inner halo, the morphology of the color-magnitude (C-M) array depends on abundance, while for clusters in the outer halo there is a great diversity of c-m morphology at a given abundance.

Figure 10 summarizes the significant facts. For clusters presently located in different zones of galactocentric distance, we have plotted [Fe/H] against a parameter that measures the color distribution on the horizontal branch. The points representing the clusters of our survey are supplemented by points representing other clusters with first-rate abundance determinations, as well as points based on Kukarkin's abundance estimates. The quantity $B/(B + R)$ was introduced by Mironov (1972); here B is the number of horizontal-branch stars bluer than the RR Lyrae gap and R is the number of horizontal-branch stars redder than the gap. For all clusters plotted in Figure 10, we have assessed this parameter from published color-magnitude arrays.

For clusters of the inner halo there is a fair correlation between $B/(B + R)$ and [Fe/H]. For clusters of the outer halo, these quantities are essentially uncorrelated. At a given low metal abundance, at say [Fe/H] $= -1.5$, the clusters of the inner halo show very little dispersion in horizontal-branch color distribution; whereas, at the same metal abundance, the clusters of the outer halo show an enormous spread. If there are two parameters governing the morphology of the color-magnitude arrays, those two parameters must be closely correlated for clusters of the inner halo and at most very loosely correlated for the clusters of the outer halo.

It is not, of course, strictly correct to regard the clusters that happen now to be in the inner or in the

outer halo as belonging to distinct populations. Some clusters now in the outer halo have traveled and will again travel through the inner halo. The justification for ignoring this mixing, which must take place, is the high probability that a cluster will be observed when it is in the neighborhood of its apogalacticon. If $\mathfrak{M}(r)$ is the galactic mass within galactocentric radius r, simple models with $\mathfrak{M}(r)$ independent of r and with $\mathfrak{M}(r)$ proportional to r show that for orbital eccentricities in the range $0.5 \leq e \leq 1.0$ a cluster spends 50% of its time at distances $r > 0.5r_a$, and 85% of its time with $r > 0.3r_a$, where r_a is its apogalactic distance. Actually, as Racine and Harris (1975) have shown, the clusters of the outer halo have unusually *large* angular momentum per unit mass and their orbits are not highly eccentric. Only a small fraction of the clusters now observed to be in the inner halo can belong to a population with apogalactica located in the outer halo.

We conclude, then, that the population of clusters that have unusually blue horizontal branches for their metal abundances are, on average, more tightly bound than the population of clusters that have unusually red horizontal branches for their metal abundances. We emphasize that clusters of *both* populations coexist in the outer halo. The remote clusters and dwarf spheroidal satellites of the Galaxy also include members of both populations; the Draco system has a predominantly red horizontal branch (Baade and Swope 1961), while the Ursa Minor system has a predominantly blue horizontal branch (van Agt 1967). Among the systems with $r > 30$ kpc, red-dominated horizontal branches are in a majority, so that, in the ratio of these two populations, there appears to be a systematic trend with galactocentric distance.

c) *The Abundance Distribution in the Outer Halo*

Any adequate theory of the origin of the clusters in the outer halo must account not only for the great range in cluster abundances found at all distances but also for the observed form of the abundance distribution. Since there is no evidence for an abundance gradient in the outer halo, we shall treat all clusters with $r > 8$ kpc together in estimating this abundance distribution.

It would be usual, perhaps, to present the observed abundance distribution in the form of a histogram, which may be regarded as the sum of a number of "unit histograms." Each unit histogram is the representation of a single data point and is located at the appropriate binning point. Familiarity obscures the crudeness of such a representation; better methods are available (e.g., Boneva, Kendall, and Stefanov 1971). The binning obviously distorts the data and a better approximation to the distribution function must clearly result from locating each unit histogram where it actually belongs. It is tempting, while we are at it, to knock the corners off the unit representation by replacing it with, for example, a unit Gaussian. If z_j with $j = 1 \cdots N$ are the abundances in the N clusters of a random sample drawn from the distribution with density $f(z)$, then a nonparametric estimate of $f(z)$ is given by the generalized histogram

$$f(z) \sim \varphi(z) = N^{-1} \sum_i K(z - z_i), \qquad (11)$$

where $K(x)$ is the Gaussian of unit area located at $x = 0$. In forming the generalized histogram, the choice of the dispersion is one of convenience, to be based on the sample density, just as is the bin width in the conventional histogram. To avoid fictitious non-zero probabilities for negative abundances, the distribution z_i should be reflected in a point $z = 0$ before applying the convolution. One advantage of such a nonparametric estimate is that when one comes to compare the data with theoretical predictions of $f(z)$ one can apply *exactly the same convolution* to the predicted distribution as has been applied to the observations.

Figure 11 shows three halo abundance distributions estimated in this way, adopting $\sigma = 0.02z_\odot$. Our sample of clusters in the outer halo consists of 15 clusters with $r > 8$ kpc and yields the probability density function shown by the solid line in Figure 11. It is obvious that the behavior near the origin is not well determined, but for $z > 0.02z_\odot$ the indication is that $f(z)$ declines exponentially with z. A larger sample of 29 clusters, which includes all those located in the outer halo for which quantitative abundance estimates exist, yields the dashed line in Figure 11.

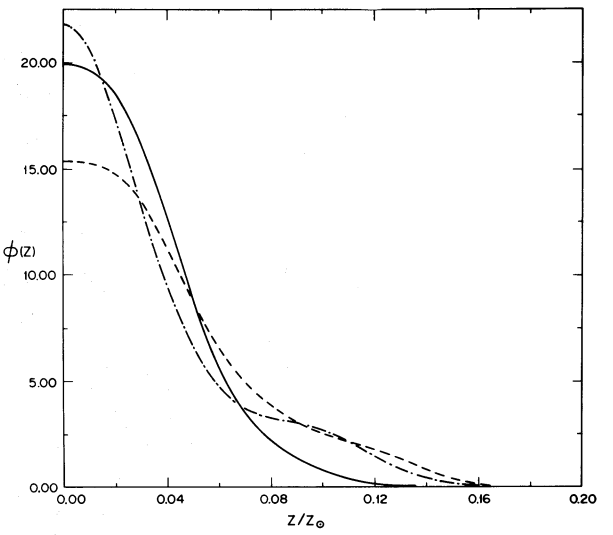

FIG. 11.—The abundance distribution of three halo samples. The curves show estimates of empirical probability density functions obtained as outlined in the text. The solid line refers to the clusters studied in this paper that have galactocentric distances exceeding 8 kpc. The dashed line refers to a larger sample of outer halo clusters, including clusters with abundances of lower accuracy. The dash-dot curve refers to a sample of halo subdwarfs. The samples are defined in the text. The three distributions are in fair agreement; the empirical probability density function declines roughly exponentially with increasing z.

This distribution, although based upon more clusters, is presumably less accurate, since, particularly at the low abundance end, accurate abundance determinations are clearly needed for a density determination. The clusters of the outer halo are simply not numerous enough to determine the behavior of the density distribution near its origin. If the density behaved exponentially over its entire range, the expected number of clusters with [Fe/H] < -1.9 and with [Fe/H] < -2.2 would be four and two, respectively, in our accurate sample of 15; this is to be compared with four and zero observed. With further observations the sample could be roughly doubled and in a complete sample of the clusters of the outer halo the expected number of clusters with [Fe/H] < -3.0 is zero if the density remains exponential for arbitrarily small z. The observed distributions, although compatible with the hypothesis of random sampling from an exponential density distribution, certainly do not rule out the possibility that cluster formation began from material with a small but nonzero metal content.

For comparison, we show the distribution over abundance computed for those subdwarfs in Sandage's (1969) paper that have $\delta(U - B) \geq 0.18$ and orbital eccentricities greater than 0.5. These are surely halo subdwarfs.[2] To convert $\delta(U - B)$ into metal abundance, we used the relation of Wallerstein (1962). The subdwarfs were selected from proper-motion surveys and are a highly biased sample, kinematically. If abundance and kinematics were correlated for this sample, the abundances would also be highly biased. Only if, as we have concluded, abundance and kinematics are actually uncorrelated could we expect this abundance distribution to reflect a property of the halo. In fact, one sees that the subdwarf distribution is remarkably similar to that derived from the sample of clusters with accurate abundances.

The three distributions are in fair agreement and we assume that they are representative of halo stars and clusters with apogalactic distances exceeding 8 kpc. The distribution is approximately exponential in form. The mean metal abundance of objects in the outer halo is $\langle z \rangle = 0.04 z_\odot$. Roughly 70% of them are more metal-deficient than $z = 0.05 z_\odot$, which corresponds to $\delta(U - B) \geq 0.21$.

d) *Summary*

Figures 9, 10, and 11 summarize the available empirical evidence on the characteristics of the cluster system of the outer halo. The main facts are that the clusters show a roughly exponential distribution over abundance (Fig. 11) that is apparently uncorrelated with galactocentric distance (Fig. 9) and that they show differences in the morphology of their color-magnitude diagrams that are uncorrelated with metal abundance—in this respect differing from more tightly bound but equally metal-poor clusters (Fig. 10).

[2] The few metal-poor subdwarfs in the solar neighborhood with orbital eccentricities less than 0.5 are presumably the primordial stars of the galactic disk. Interestingly, they appear to have a distribution over metal abundance different from the halo subdwarfs. This makes it unlikely that they are halo subgiants that have been misidentified as subdwarfs.

IX. THE CLUSTER SYSTEM AND THE FORMATION OF THE HALO

The properties of the system of halo clusters, which are among the oldest objects that constitute the Galaxy, are clues to the processes involved in its formation. It is of interest to compare these properties with the implications of some simple conceptual schemes for the formation of the Galaxy. In doing so, we shall consider only those schemes that are in the tradition of Kant's (1755) conjecture that the Galaxy collapsed from a more dispersed state under the influence of its self-gravity. Recent developments in the study of galaxy formation are reviewed by Gott (1977) and Larson (1976).

a) *Inferences from the Lack of a Gradient in the Outer Halo*

It is a familiar idea that, in the slow contraction of a pressure-supported galaxy undergoing star formation and chemical enrichment, an abundance gradient will arise, and persist, in the stellar component that condenses out of the contracting gas cloud. In a stellar system formed in such a process, both the mean metal abundance and the range in metal abundance are expected to decrease with increasing galactocentric distance. This is so whether the protogalaxy is well mixed or not. One implication of the lack of a gradient in the outer halo is that the globular clusters did not form in such a pressure-supported slow collapse.

The situation is essentially different if the collapsing gas is freely falling. If chemical enrichment brings the metal abundance up to a level z_f at the epoch when free-fall conditions come to an end, we should expect clusters with all metal abundances $0 \leq z \leq z_f$ to occur within the protogalaxy at that epoch and to be freely falling. Their kinematic properties will be independent of their abundances, so that no gradient can be expected for clusters in this abundance range in a cluster system formed by such a process. One possible inference from Figure 9 is, therefore, that all clusters in the Galaxy more metal-poor than $z = 0.1 z_\odot$ were formed during the free-fall phase of the galactic collapse. Eggen, Lynden-Bell, and Sandage (1962) concluded, from a study of the kinematics and abundances of high-velocity stars in the solar neighborhood, that *stars* within this abundance range *were* formed in the free-fall phase of the galactic collapse. If this is correct, one would not expect them to exhibit a gradient.

The picture of the clusters that now constitute the outer halo forming from freely falling gas is consistent with the observed lack of a gradient, but it is more specific than the observations really demand. The minimum requirement seems to be that these clusters were formed in such a way that, when they came into dynamical equilibrium with the galactic system, their kinematic properties were uncorrelated with their abundances. For example, these clusters could have

formed in a number of small protogalaxies that subsequently merged to form the present galactic halo.

b) *Inferences from the Galactic Distribution of the Second Parameter*

To avoid arbitrary hypotheses, we shall suppose that the morphology of the color-magnitude array of a cluster is determined by its age and composition alone. It is well known from earlier work (e.g., Faulkner 1966; Rood and Iben 1968; Simoda and Iben 1970; Castellani and Tornambe 1977) that the diversity of horizontal-branch color distribution can be accounted for by one of three factors: (*a*) by an age spread of $\sim 10^9$ years; (*b*) by a spread in helium abundance amounting to $\Delta Y \sim 0.05$; or (*c*) by a spread in C, N, O abundance by a factor of 2 to 3.

If we assume, as is often done, that the spread in cluster age is negligibly small, then Figure 10 implies that the metal-poor clusters of the inner halo must be helium-rich (or, equivalently CNO-poor) with respect to some (but not all) of the metal-poor clusters of the outer halo. We would need to assume that enrichment in the metals occurred in separate events from helium (or CNO) enrichment. The occurrence of these different kinds of events would need to be uncorrelated in the outer region of the Galaxy. None of this is particularly implausible; but, on this hypothesis, one also requires an *additional* mechanism to account for the fact that metal abundance and helium (or CNO) abundance *are* well correlated for the metal-poor clusters of the inner halo. Perhaps such a mechanism could be devised, but we have been unable to think of one that is very convincing.

What if age is, after all, the second parameter? Then Figure 10 shows that the loosely bound clusters are those with a large age spread, while the tightly bound clusters of the inner halo have a negligible age spread. It is not difficult to imagine, in a general way, how this might come about. In the collapse of a centrally concentrated gaseous protogalaxy, the central regions will collapse rapidly and star formation in these regions will produce a tightly bound system. The outer fringes will fall in over a longer period of time and the stars formed out of them will remain in a more loosely bound outer halo.[3] Inhomogeneous collapses of this kind have been discussed by Larson (1974), by Gott (1975), and by Gott and Thuan (1976).

To account for the diversity of horizontal-branch morphology, an age spread of $\sim 10^9$ years is required. Our observation requires, then, on this hypothesis, that the collapse time for the clusters of the inner halo is less than 10^9 years while that for the cluster system of the outer halo exceeds 10^9 years. Sandage (1970) writes the free-fall equation in the form

$$T_{\text{collapse}} = 0.6 \times 10^9 (D/50\ \text{kpc})^{3/2} \times (10^{11} \mathfrak{M}_\odot / \mathfrak{M}_{\text{eff}})^{1/2}\ \text{years}, \quad (12)$$

where D is the galactocentric distance from which the collapse commenced and $\mathfrak{M}_{\text{eff}}$ is the galactic mass interior to this distance. The collapse of the inner halo must, therefore, have taken place on a time scale of $\sim 10^8$ years and, if the outer halo clusters accumulated over a period exceeding 10^9 years, the gas from which they formed must have fallen in from great distances—say, distances of order 100 kpc.

Now, most of the clusters that constitute the outer halo have apogalactic distances that are much smaller than 100 kpc. The question is, then, Could they, nevertheless, have formed out of gas that fell in from distances as great as 100 kpc? Obviously not, if the clusters formed out of gas in free fall; but perhaps so if some dissipation of the energy of infall occurred before the clusters formed. This does not seem at all unlikely; indeed, it is difficult to imagine how clusters can form without some dissipation occurring. Binney (1976) has imagined that the sites of earliest star formation in a collapsing protogalaxy are the transient sheets of gas generated by the collision of infalling gas flows. Such collisions dissipate the kinetic energy of infall. If the formation of the globular clusters of the outer halo takes place in such an environment, there appears to be no reason why cluster formation could not continue over several times 10^9 years and yet produce a cluster system whose formal collapse time, as judged by equation (12), is an order of magnitude smaller.

From the galactic distribution of the second parameter, we make the tentative inference that the second parameter is, in fact, age, and conclude that the clusters of the outer halo formed before they came into dynamical equilibrium with the Galaxy but after the infalling gas from which they formed had dissipated much of its kinetic energy. We hypothesize that these clusters originate in transient gaseous condensations in the formation of which the dissipation occurs.

c) *Inferences from the Abundance Distribution of Outer Halo Objects*

It is interesting to compare the abundance distributions of Figure 11 with those predicted by the simple model of galactic chemical evolution (Searle and Sargent 1972; Searle 1972). In a homogeneous and closed system that is initially without either stars or metals, if the yield y is constant, then, at any subsequent epoch, the metal abundance z is given by

$$z = y \ln (1/x), \quad (13)$$

where x is the fraction of the mass of the system which, at that epoch, remains in the form of gas. If $F(z)$ is the fraction of stars formed before the epoch

[3] Of course, on this hypothesis, at any epoch a small fraction of the loosely bound clusters will be located within the inner regions of the Galaxy. Clusters with apogalactica greater than 15 kpc will penetrate to within 5 kpc of the galactic center if their orbital eccentricities exceed 0.5; such clusters will spend less than 15% of their time in these inner regions.

when $x = x_1$ and $z = z_1$ that are more metal-poor than z, then

$$F(z) = (1 - x)/(1 - x_1) . \quad (14)$$

From equations (13) and (14) the probability density $f(z)$ follows:

$$f(z) = (1/y) \exp(-z/y) \quad (z \leq z_1)$$
$$= 0 \quad \text{(otherwise)} . \quad (15)$$

There are two limiting forms to this abundance distribution. If only a very small fraction of the system has been converted into stars so that $x_1 \approx 1$, then $z \ll y$ and $f(z)$ is constant for $z \leq z_1$. In terms of $\langle z \rangle$, the average abundance of the stars formed, in this limit

$$f(z) = 1/(2\langle z \rangle) , \quad z \leq 2\langle z \rangle . \quad (16)$$

The opposite limit obtains when the system has evolved to completion, i.e., $x_1 \approx 0$. In this case

$$f(z) = (1/\langle z \rangle) \exp(-z/\langle z \rangle) . \quad (17)$$

These limiting distributions of the simple model are compared with the observations in Figure 12. The solid line is the halo abundance distribution. It has been recomputed, using the method of § VII*c*, adopting $\sigma = 0.015 z_\odot$, and combining the data for all 29 clusters and all 37 halo subdwarfs. Since our method of obtaining the density function involves convolution of the data with a Gaussian, we have convolved the distributions of equations (16) and (17) with the same Gaussian before displaying them in Figure 12. They are shown by the dotted and dashed lines, respectively.

The distribution predicted by the simple model in the limit of small evolution does not fit the observations at all, while that predicted for a system that has evolved to completion provides an astonishingly good fit. *If the protogalaxy evolved in a homogeneous way with constant yield*, the implication is that it evolved to completion, the gas being completely converted into stars during the halo-forming phase. At this epoch the yield must have been low, equaling the mean z of the halo stars or $0.04 z_\odot$. On this picture the gas from which the disk of the Galaxy formed must have resulted from the mass loss of evolved halo stars.

This picture seems unlikely to us, because if star formation goes to completion in the halo-forming phase of a spiral galaxy, what is it that differentiates spiral and elliptical galaxies? Sandage, Freeman, and Stokes (1970), Larson (1976), and Gott and Thuan (1976) persuasively argue that in the spirals only a small fraction of the collapsing gas goes to make stars during the collapse phase. If this is correct, then the assumption of a closed system is probably inappropriate to the conditions under which the clusters of the outer halo formed. A similar conclusion was reached by Hartwick (1976), who was the first to estimate the halo abundance distribution[4] and to discuss its origin. Hartwick suggested that the way out of the difficulty was to allow for temporary removal of gas from the star-forming process.

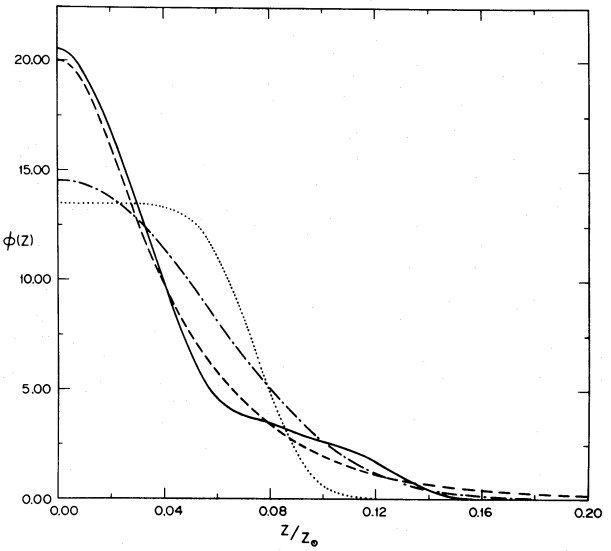

FIG. 12.—Observed and theoretical abundance distributions. The solid line is an empirical probability density function obtained from a sample of halo clusters and subdwarfs. The dash-dot curve is the prediction of the $\mu = 5$ case of Searle's (1977) stochastic model. The dotted curve is the prediction of the simple model of galactic evolution in the limit of negligible gas consumption. The dashed curve, which provides a close fit to the observed one, is the prediction of the simple model in the limit of complete gas consumption. The theoretical distributions have been subjected to the same convolution that was used in estimating the empirical one.

If, as we have suggested, the clusters of the outer halo originated in transient condensations and were accreted over a span of time longer than the dynamical time scale, it may be inappropriate to compare their abundance distribution with the predictions of a closed, homogeneous model. It may be a better idealization of a complex situation to think of the process of halo formation as the merging of a number of distinct subsystems. Such subsystems, which we shall call fragments, may perhaps be thought of as having the character of small gas-rich irregular galaxies. Fragments of this sort, we suggest, provide the natural context for the process proposed by Hartwick.

Chemical evolution in a system of merging fragments has previously been considered by Searle (1977), who proposed a stochastic model to account for the observed halo abundance distribution. In this model each fragment makes a few clusters and then *suddenly* loses its remaining gas as a result of disruption by internal supernova explosions or as a result of its

[4] Hartwick derived cluster abundances from Kukarkin's (1974) estimates and approximated the distribution by a Gaussian in [Fe/H]. In such a treatment the closeness of the agreement between the observed distribution and that predicted by the simple model in the limit of complete gas consumption is obscured.

sweeping through the galactic plane. The best-fitting case is shown in Figure 12. Fragment evolution with *gradual* gas loss gives a still better fit to the observations. Imagine chemical enrichment proceeding in a well-mixed and initially metal-poor system that gradually loses gas as it evolves. This gas loss may be thought of as resulting from disruption by supernova explosions occurring within the fragment or as resulting simply from the ablation of the fragment. Suppose, following Hartwick, that the gas-loss rate is proportional to the rate at which stars form. Under these circumstances, equations (13)–(17) remain unchanged; x is now to be interpreted as the fraction of the initial mass of the fragment remaining within it in gaseous form, while the nuclear yield y is replaced in the equations by an effective yield $y_{\rm eff}$, that is related to y by

$$y_{\rm eff} = y/(1 + \alpha)\,, \qquad (18)$$

where α is the ratio of the gas-loss rate to the rate of gas consumption by star formation.

The main point here is that a fragment evolving to completion in this way will produce stars and clusters with the exponential abundance distribution of equation (17), even though only a small fraction of the fragment mass is converted into stars. The mean metal abundance, $\langle z \rangle$, of the stars formed will equal $y_{\rm eff}$, and, according to equation (18), will depend on α, the ratio of gas lost to stars formed. The basic idea that galaxy evolution with gas loss leads to the production of metal-poor systems was originally suggested by Sandage (1965) as an explanation for the properties of the dwarf spheroidal satellites of the Galaxy. This process is, we suggest, also responsible for the metal deficiency of the Small Magellanic Cloud. We infer from the roughly exponential form of the observed abundance distribution that the clusters of the outer halo originated within fragments that, in a similar manner, gradually lost gas while they underwent chemical evolution.

d) Conclusions regarding Galactic Evolution

The properties of the cluster system of the galactic halo resulting from the abundance study reported in this paper have been summarized in § VIII*d*. In attempting to account for these properties, we have been led, in each case, away from the notion of an isolated, uniform, homogeneous, collapsing protogalaxy. The observations appear to indicate a more chaotic origin for the Galaxy. An explanation of the properties of the outer halo requires the formulation of a hypothesis regarding the circumstances under which the globular clusters of the outer halo formed. It is in the nature of cosmogony that this hypothesis has to be more impressionistic than we should like.

We tentatively propose that the gas from which the clusters and stars of the outer halo formed continued to fall into the Galaxy for some time after the collapse of its central regions had been completed; that the interactions of the infalling gas dissipated much of its kinetic energy and gave rise to transient high-density regions in which the halo stars and clusters formed; that these regions dispersed even while they underwent chemical evolution; that the stars and clusters that had formed within them eventually fell into dynamical equilibrium with the Galaxy and constitute its present outer halo, while the gas lost from these protogalactic star-forming regions was eventually swept into the galactic disk.

We are grateful to Allan Sandage for making photometric results and finding charts available to us prior to publication and to Althea Wilkinson for invaluable help with problems of data reduction.

REFERENCES

Arp, H. C. 1955, *A.J.*, **60**, 317.
———. 1962, *Ap. J.*, **135**, 311.
Arp, H. C., and Hartwick, F. D. A. 1971, *Ap. J.*, **167**, 499.
Arp, H. C., and Johnson, H. L. 1955, *Ap. J.*, **122**, 171.
Baade, W., and Swope, H. H. 1961, *A.J.*, **66**, 300.
Barbon, R. 1965, *Asiago Obs. Contr.*, No. 175.
Baum, W. A. 1954, *A.J.*, **59**, 422.
Bessell, M. S., and Norris, J. 1976, *Ap. J.*, **208**, 369.
Binney, J. 1976, *M.N.R.A.S.*, **177**, 19.
Boneva, L. I., Kendall, D. G., and Stefanov, I. 1971, *J. Roy. Stat. Soc. B*, **33**, 1.
Butler, D. 1975, *Ap. J.*, **200**, 68.
Canterna, R. 1975, *Ap. J.* (*Letters*), **200**, L63.
Cathey, L. R. 1974, *A.J.*, **79**, 1370.
Castellani, V., and Tornambe, A. 1977, *Astr. Ap.*, **61**, 427.
Ciardullo, R. B., and Demarque, P. 1977, *Trans. Astr. Obs. Yale University*, Vol. **33**.
Cohen, J. G. 1978, preprint.
Cohen, J. G., Frogel, J. A., and Persson, S. E. 1978, *Ap. J.*, **222**, 165.
Cowley, A. P., Hartwick, F. D. A., and Sargent, W. L. W. 1978, *Ap. J.*, **220**, 453.
Cuffey, J. 1961, *A.J.*, **66**, 71.
———. 1965, *A.J.*, **70**, 732.
Dickens, R. J. 1972, *M.N.R.A.S.*, **157**, 281.
Dickens, R. J., and Bell, R. A. 1976, *Ap. J.*, **207**, 506.
Dickens, R. J., and Rolland, A. 1972, *M.N.R.A.S.*, **160**, 37.
Eggen, O. J., Lynden-Bell, D., and Sandage, A. R. 1962, *Ap. J.*, **136**, 748.
Faulkner, J. 1966, *Ap. J.*, **144**, 978.
Gott, J. R. 1975, *Ap. J.*, **201**, 296.
———. 1977, *Ann. Rev. Astr. Ap.*, **15**, 235.
Gott, J. R., and Thuan, T. X. 1976, *Ap. J.*, **204**, 649.
Graham, J. A. 1975, *Pub. A.S.P.*, **87**, 641.
———. 1977, *Pub. A.S.P.*, **89**, 425.
Harris, W. E. 1975, *Ap. J. Suppl.*, **29**, 397.
———. 1976, *A.J.*, **81**, 1095.
Harris, W. E., and Racine, R. 1973, *A.J.*, **78**, 242.
Harris, W. E., Racine, R., and de Roux, J. 1976, *Ap. J. Suppl.*, **31**, 13.
Hartwick, F. D. A. 1976, *Ap. J.*, **209**, 418.
Hartwick, F. D. A., and McClure, R. D. 1972, *Ap. J.* (*Letters*), **176**, L57.
Hesser, J. E., Hartwick, F. D. A., and McClure, R. D. 1977, *Ap. J. Suppl.*, **33**, 471.
Johnson, H. L., and Sandage, A. R. 1956, *Ap. J.*, **124**, 379.
Kadla, Z. I. 1966, *Comm. Pulkova Obs.*, No. 181, **24**, 93.
Kant, I. 1755, *Universal Natural History and Theory of the Heavens*, ed. and transl. W. Hastie (1969; Ann Arbor: University of Michigan Press).
Kinman, T. D. 1959, *M.N.R.A.S.*, **119**, 538.
Kukarkin, B. B. 1974, *The Globular Star Clusters* (Moscow: Nauka).
Larson, R. B. 1974, *M.N.R.A.S.*, **166**, 585.

Larson, R. B. 1976, in *Galaxies*, ed. L. Martinet and M. Mayor (Geneva: Geneva Observatory), p. 67.
Mayall, N. V. 1946, *Ap. J.*, **104**, 290.
McClure, R. D., and Norris, J. 1977, *Ap. J.* (*Letters*), **216**, L101.
Miller, J., and Mathews, W. 1972, *Ap. J.*, **172**, 593.
Mironov, A. V. 1972, *Soviet Astr.—AJ*, **16**, 105.
Morgan, W. W. 1956, *Pub. A.S.P.*, **68**, 509.
Norris, J., and Zinn, R. 1977, *Ap. J.*, **215**, 74.
Oke, J. B., and Schild, R. 1970, *Ap. J.*, **161**, 1015.
Osborn, W. 1971*a*, *Observatory*, **91**, 223.
———. 1971*b*, Ph.D. thesis, Yale University.
Racine, R., and Harris, W. E. 1975, *Ap. J.*, **197**, 147.
Rood, R., and Iben, I. 1968, *Ap. J.*, **154**, 215.
Sandage, A. R. 1965, in *The Structure and Evolution of Galaxies, Solvay 1964* (London: Interscience), p. 83.
———. 1969, *Ap. J.*, **158**, 1115.
———. 1970, *Ap. J.*, **162**, 841.
Sandage, A. R., Freeman, K. C., and Stokes, N. R. 1970, *Ap. J.*, **160**, 831.
Sandage, A., and Hartwick, F. D. A. 1977, *A.J.*, **82**, 459.
Sandage, A., Katem, B., and Johnson, H. L. 1977, *A.J.*, **82**, 389.
Sandage, A. R., and Walker, M. F. 1955, *A.J.*, **60**, 230.
———. 1966, *Ap. J.*, **143**, 313.
Sandage, A. R., and Wildey, R. 1967, *Ap. J.*, **150**, 469.
Savedoff, M. P. 1956, *A.J.*, **61**, 254.
Searle, L. 1972, in *Stellar Ages, IAU Colloq. No. 17*, ed. M. Delplace and G. Cayrel de Strobel (Paris: Meudon Observatory).
———. 1977, in *The Evolution of Galaxies and Stellar Populations*, ed. B. M. Tinsley and R. B. Larson (New Haven: Yale University Observatory), p. 219.
Searle, L., and Sargent, W. L. W. 1972, *Ap. J.*, **173**, 25.
Simoda, M., and Iben, I. 1970, *Ap. J. Suppl.*, **22**, 81.
van Agt, S. 1967, *Bull. Astr. Inst. Netherlands*, **19**, 275.
van den Bergh, S. 1967, *A.J.*, **72**, 70.
Wallerstein, G. 1962, *Ap. J. Suppl.*, **6**, 407.
Woltjer, L. 1975, *Astr. Ap.*, **42**, 109.
Zinn, R. 1977, *Ap. J.*, **218**, 96.

LEONARD SEARLE and ROBERT ZINN: Hale Observatories, 813 Santa Barbara St., Pasadena, CA 91101